Design and Synthesis of Oligopeptidic Parvulin Inhibitors

Nicola Relitti[+],[a, e] A. Prasanth Saraswati[+],[a, f] Gabriele Carullo,[a] Alessandro Papa,[a] Alessandra Monti,[b] Rosaria Benedetti,[c] Eugenia Passaro,[c] Simone Brogi,[d] Vincenzo Calderone,[d] Stefania Butini,[a] Sandra Gemma,[a] Lucia Altucci,[c] Giuseppe Campiani,*[a] and Nunzianna Doti*[b]

Pin1 catalyzes the *cis-trans* isomerization of pThr-Pro or pSer-Pro amide bonds of various proteins involved in several physio/pathological processes. In this framework, recent research activity is directed toward the identification of new selective Pin1 inhibitors. Here, we developed a set of peptide-based Pin1 inhibitors. Direct-binding experiments allowed the identification of the peptide-based inhibitor **5k** (methylacetyl-L-alanyl-L-histidyl-L-prolyl-L-phenylalaninate) as a potent ligand of Pin1. Notably, **5k** binds Pin1 with higher affinity than Pin4. The comparative analysis of molecular models of Pin1 and Pin4 with the selected compound gave a rational explanation of the biochemical activity and pinpointed the chemical elements that, if opportunely modified, may further improve inhibitory potency, pharmacological properties, and selectivity of future peptide-based parvulin inhibitors. Since **5k** showed limited cell penetration and no antiproliferative activity, it was conjugated to a polyarginine stretch (R8), known to promote cell penetration of peptides, to obtain the **R8–5k** derivative, which displayed antiproliferative effects on cancer cell lines over non-tumor cells. The effect of R8 on cell proliferation was also investigated. This work warrants caution about applying the R8 strategy in the development of cell-penetrating antiproliferative peptides, as it is not inert.

Introduction

In the superfamily of molecular chaperones, peptidyl-prolyl *cis-trans* isomerases (PPIase) represent unique members since they do not use cofactors, such as ATP, to promote their activity, but they rather bind to target proteins through conformational

[a] Dr. N. Relitti,[+] Dr. A. Prasanth Saraswati,[+] Dr. G. Carullo, A. Papa, Prof. S. Butini, Prof. S. Gemma, Prof. G. Campiani
Department of Biotechnology, University of Siena
Via Aldo Moro 2, 53100 Siena (Italy)
E-mail: giuseppe.campiani@unisi.it

[b] Dr. A. Monti, Dr. N. Doti
Institute of Biostructures and Bioimaging
National Research Council, 80131 Naples (Italy)
E-mail: nunzianna.doti@cnr.it

[c] Dr. R. Benedetti, E. Passaro, Prof. L. Altucci
Department of Precision Medicine
University of Campania Luigi Vanvitelli
80138 Naples (Italy)

[d] Prof. S. Brogi, Prof. V. Calderone
Department of Pharmacy
University of Pisa, 56126 Pisa (Italy)

[e] Dr. N. Relitti[+]
Current address: IRBM Science Park
Via Pontina km 30,600
00071 Pomezia, Rome (Italy)

[f] Dr. A. Prasanth Saraswati[+]
Current address: Department of Basic Medical Sciences
Purdue College of Veterinary Medicine
West Lafayette, IN, 47907 (USA)

[+] These authors contributed equally to this work.

Supporting information for this article is available on the WWW under https://doi.org/10.1002/cmdc.202200050

changes that interfere with proline isomerization.[1] Among the various subfamilies, Parvulins represent the smallest family of PPIases, comprising NIMA interacting protein 1 (Pin1) and parvulin-14 (Par14), also known as Pin4. Pin1 encompasses a *C*-terminal phosphorylation-dependent catalytic domain and a *N*-terminal WW domain, and catalyzes the *cis-trans* isomerization of pThr-Pro or pSer-Pro amide bonds of substrate proteins.[2] Pin1 is the only enzyme that catalyzes the isomerization of phosphorylated substrates in humans.[3] By altering the ratio of *cis-trans* conformers of phosphorylated proteins, Pin1 can regulate several kinase signaling processes. Some of the important Pin1 substrates include cyclin D1, NF-κB, and p53.[4–6] Overexpression of Pin1 is implicated in various types of cancers, including hepatic, esophageal, rectal, and prostatic cancers.[7] Owing to the critical role of Pin1 in cell cycle regulation, with increased expression in cancers, it represents an attractive target for developing new chemotherapeutic agents.[8] Pin4 has been found in both the cytosol and the nucleus. It lacks the basic pocket needed for selection of pSer/Thr-Pro substrates.[1] Pin4 presents the conserved isomerase and chaperoning activity characteristic of most PPIases; nevertheless, the exact cellular functions remain cryptic. Of note, Pin4 associates with insulin receptor substrate 1 (IRS-1), enhancing insulin-induced IRS-1 phosphorylation and metabolic functions.[9] The PPIase domains of Pin1 and Pin4 show 35% sequence identity and more than 50% homology. The loop regions are different in terms of length between β1 and α1 (extended in Pin1) as well as between α3 and β3 (extended in Pin4).[10] There is also a long basic loop in these isoforms, which serves as a substrate binding site and isomerization catalytic site in Pin1, while in Pin4 the function remains unclear. Phosphorylation of Ser7 and Ser9 of Pin4 by the PKB/Akt kinase in a Crm1-dependent

ChemMedChem

Research Article
doi.org/10.1002/cmdc.202200050

**Chemistry
Europe**
European Chemical
Societies Publishing

pathway, regulated by 14-3-3 protein, promotes the migration of phosphorylated Pin4 from the nucleus to the cytosol. Cytoplasmic localization contributes to silence protein's function initiating proteasomal degradation.[10] Additionally, Pin4 does not accelerate the *cis-trans* interconversion of *p*Ser/Thr-Pro bonds typical of Pin1 preferring Arg–Pro moieties.[11] Pin4 is phosphorylated at Tyr122 in tumor cells expressing the fusion protein F3-T3, promoting the formation of a F3-T3-Pin4 axis, responsible of an increased oxidative stress in cancer cells.[12,13] Medicinal chemistry research is now moving toward the development of small peptides that could mimic physiological behaviors.[14] This holds true with regards to the synthesis of potential Parvulin inhibitors.

Accordingly, the protected peptide Suc–Ala–Glu–Pro–Phe-*p*Nitroanilide (**1**, Figure 1) was developed as a potential Pin1 inhibitor, prototypic of a new class of potential anticancer agents.[15] Non-peptidic small-molecule Pin inhibitors include Juglone (**2**), PiB (**3**), halogenated phenyl-isothiazolone (TME-001, **4**) (Figure 1). The best results in terms of selective Pin1 inhibition were obtained in cancer cells using novel biomimetic cyclic peptides more potent than small-molecule inhibitors, since these latter lack significant effectiveness and/or specificity.[15] Indeed, most of the known Pin1 inhibitors show a weak selectivity over Pin4, that is equally overexpressed in cancer cells.[16] Nevertheless, most of the potential inhibitors of Pin1 and Pin4 so far reported have no effects in cells due to low membrane permeability.[17] The principal strategies employed for improving cell permeability of peptides may include cyclization[18,19] or conjugation with an octaarginine (R8) tag, which has been proved to favor cellular internalization.[20] In fact, cell-penetrating peptides (CPPs), such as R8, can transport into the cell a wide variety of biologically active conjugates including antiproliferative peptides.[20] This has been explained
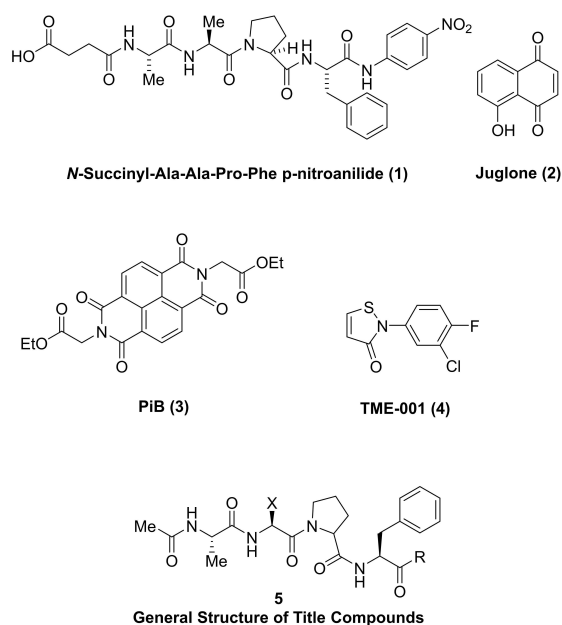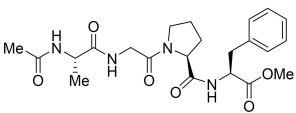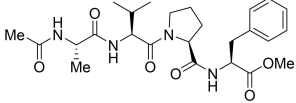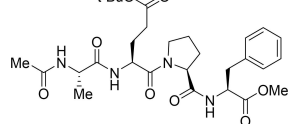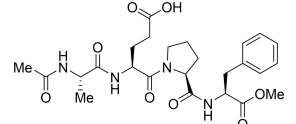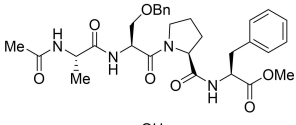
with the formation of a pore (barrel-stave), which results from the formation of bundles by amphipathic R-helical peptides.[21] R8-conjugates have been proven to penetrate both U87 and GL261 glioma cell lines, displaying sustained release and revealing minimal toxicity when administered in mice.[22] Moreover, a Smac/R8 peptide demonstrated to better accumulate into the cells, due to higher internalization, with respect to Smac alone, improving cell sensitivity to the drug.[23,24] Also in several cases, these adducts demonstrated high stability at physiological pH and an increased release of drugs. In this framework, with the aim of developing new inhibitors against Pin1, a set of new analogues of Ala–Gly–Pro–Phe (with general structure **5**; Figure 1) used as early molecular template, were designed, synthesized and functionally characterized. Molecular docking analyses were performed to highlight the differences in the binding mode of selected compounds, respect to the starting template typified by the general structure **5**, against both Pin1 and Pin4. Computational study evidenced critical structural determinants governing the activity of our compounds. In addition, to test the biological effects of new selected oligopeptides they were conjugated with a polyarginine stretch (R8) at their *N*-terminus. The new conjugates were tested to determine their inhibitory potency toward Pin1 and Pin4 as well and to determine their antiproliferative activity in cancerous A549, MCF7, HCT116, LNCaP, PNT2 and non-cancerous AC16 cell lines.

Results and Discussion

Design and synthesis of compounds

In order to identify new oligopeptide inhibitors of Pin1 protein, we designed a new set of tetrapeptides, starting from the well-known substrate of the catalytic site of PPIases (N-terminus acetylated (Ac) Ala–Gly–Pro–Phe, see **5a** in Table 1). The docked pose of **5a** in complex with Pin1 (Figure 2) showed some relevant interactions of the ligand within Pin1 binding site, targeting Arg-rich region (R68 and R69) belonging to the long loop between β1 and α1 motif, through the acetyl group of *N*-terminus and the carbonyl-group of Gly. This binding mode suggested the replacement of the Gly residue of **5a** with a series of long chained amino acids to obtain derivatives potentially able to maximize the interactions with the Pin1 binding site (Table 1). The synthesis of compounds **5a–p**, with Ac–Ala at *N*-terminus linked to different amino acids (Table 1) was accomplished by employing solution-phase synthesis. Scheme 1 describes the synthetic route to compounds **5a–o**. A convergent approach between Phe–OMe and *N*-Boc–Pro to the Pro–Phe dipeptide (**6**), followed by Boc deprotection, was performed.[25] For the synthesis of compound **9**, Ala–OMe·HCl was initially converted into Ac–Ala–OMe by using AcCl in DCM. The obtained compound was then hydrolyzed at the ester functionality to **9** in basic conditions and used in the next steps.[26] Amine **6** was used as the starting point for the coupling reaction with different amino acids to obtain compounds **7a–c,e–g,i,k,l–n**. The subsequent *N*-deprotection fur-

Figure 1. Known Pin Inhibitors (compounds **1–4**) and general structure **5** of the title compounds **5a–p**.
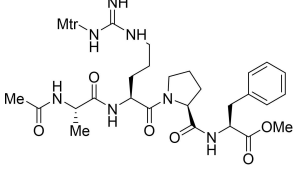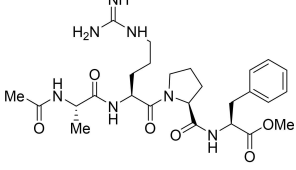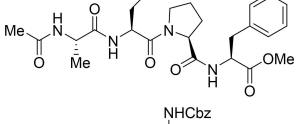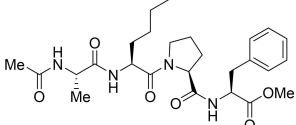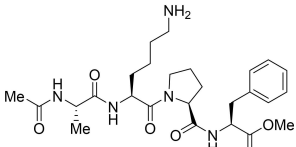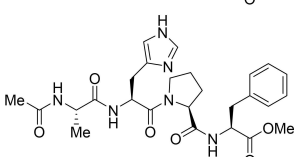
ChemMedChem

Research Article
doi.org/10.1002/cmdc.202200050

Chemistry
Europe
European Chemical
Societies Publishing

Table 1. Structures of compounds **5a–p** and their affinity for Pin1 and Pin4 enzymes.

Compd	Structure	Pin1 KD [μM][a]	Pin4 KD [μM][a]
5a		6.09 ± 4.47	N/D
5b		6.11 ± 3.74	N/D
5c		53.63 ± 18.85	N/D
5d		30.49 ± 9.03	N/D
5e		N/D	N/D
5f		N/D	18.61 ± 11.47
5g		N/D	N/D
5h		4.50 ± 2.47	N/D
5i		70.17 ± 30.70	28.19 ± 7.00
5j		22.37 ± 11.25	N/D
5k		0.45 ± 0.30	5.70 ± 2.89

ChemMedChem

Research Article
doi.org/10.1002/cmdc.202200050

Chemistry
Europe
European Chemical
Societies Publishing

Table 1. continued

Compd	Structure	Pin1 KD [μM][a]	Pin4 KD [μM][a]
5 l		14.06 ± 13.29	N/D
5 m		62.51 ± 15.85	N/D
5 n		N/D	N/D
5 o		N/D	N/D
5 p		N/D	N/D

[a] Data are the mean ± S.D. of three independent experiments; N/D: K_D values not determined or could not be accurately determined in the concentration range used.
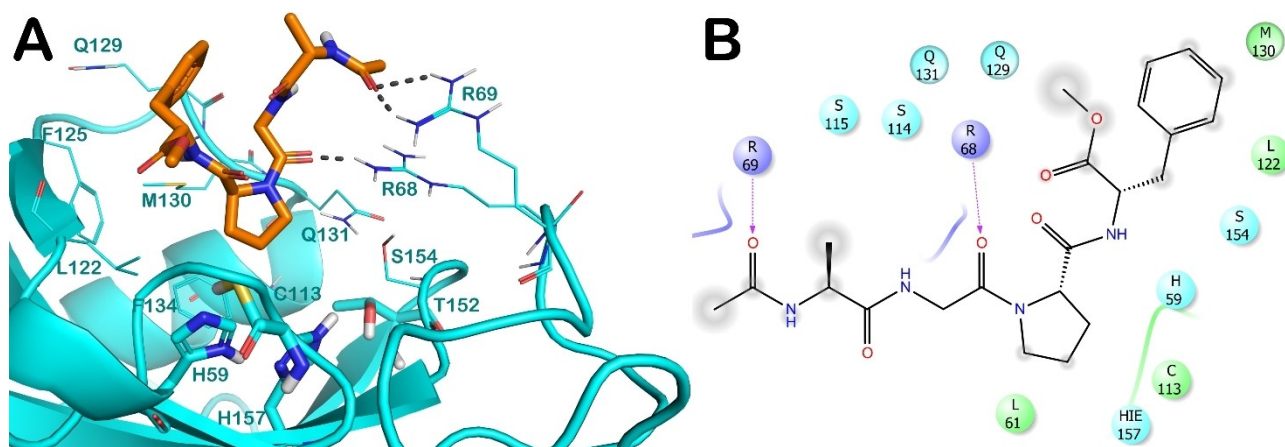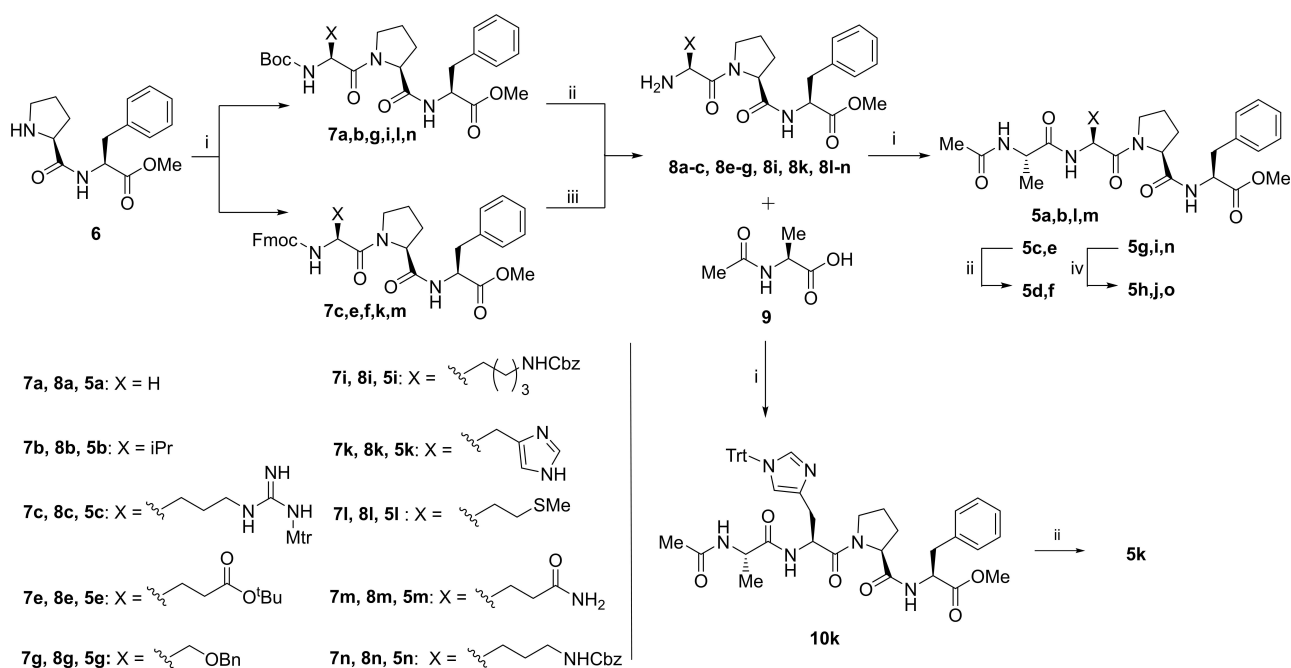

Figure 2. (A) Docked pose of compound **5 a** (orange sticks) bound to Pin1 (cyan cartoon). (B) 2D interaction diagram of **5 a** docking pose interaction with the key residues in Pin1 catalytic site. Interacting residues in the binding site are represented by lines, while the catalytic tetrads are represented by sticks (H59, H157, C113, and T152). For sake of clarity, H157 was reported as HIE157 (HIE stands for tautomeric histidine ε-nitrogen) in the ligand interaction diagram according to the protein preparation output. H-bonds are illustrated by grey dotted lines (right panel). Pictures were generated by PyMOL (The PyMOL Molecular Graphics System, v1.8; Schrödinger, LLC, New York, 2015) and by ligand interaction diagram available in Maestro.

nished intermediates **8 a**–**c**, **8 e**–**g**, **8 i**, **8 k**, **8 l**–**n**, that, coupled with **9**, furnished the compounds **5 a**–**c**, **5 e**–**g**, **5 i**, **5 l**–**n**. In the same experimental conditions, when coupled with **9**, **8 k** provided the derivative **10 k**. The removal of the *tert*-butyl group of **5 e** by exposure to TFA, gave **5 f**. With the same procedure, **5 d** was obtained starting from **5 c**. To obtain **5 k**, the Mtr group of the intermediate **10 k** was cleaved under acidic conditions. The deprotection of compounds **5 g** and **5 i** by

catalytic hydrogenation provided **5 h** and **5 j**, respectively. By using a similar approach, the compound **5 p** was obtained as reported in the Scheme 2. N-Boc-D-proline **11** was reacted with N-methyl-phenylalanine providing dipeptide **12**. The subsequent Boc removal furnished **13**, that was coupled with N^2-(acetyl-L-alanyl)-N^6-((benzyloxy)carbonyl)-L-lysine, leading to compound **15**, which underwent to a final Cbz-deprotection.

ChemMedChem

Research Article
doi.org/10.1002/cmdc.202200050

**Chemistry
Europe**
European Chemical
Societies Publishing

Scheme 1. Synthesis of oligopeptides **5a–l**. i) appropriate *N*-protected amino acids for **6**, or compound **9** for **8a–c**, **8e–g**, **8i**, **8k**, **8l–n**, EDCI, HOBt, DIPEA, dry DCM, 12 h; ii) TFA, DCM, 0 °C, 1 h; iii) piperidine, DCM, 25 °C, 3 h; iv) H$_2$, Pd/C, EtOAc/MeOH, rt, 12 h.
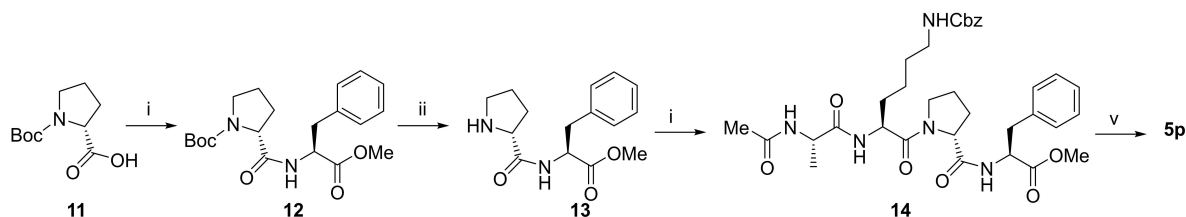
Scheme 2. Synthesis of compound **5p**. i) methyl *L*-phenylalanine for compound **11** or *N*^{2}-(acetyl-L-alanyl)-*N*^{6}-((benzyloxy)carbonyl)-*L*-lysine for compound **13**, EDCI, HOBt, DIPEA, dry DCM, 12 h; ii) TFA, DCM, 0 °C, 1 h; v) H$_2$, Pd/C, EtOAc/MeOH, rt, 12 h.

Inhibition assays and structure-activity relationships (SARs)

The ability of compounds **5a–p** to interact with the recombinant human 6His-tagged-Pin1, 6His-tagged-Pin4 (hereafter Pin1 and Pin4, respectively) was analyzed by direct-binding assays by using Enspire-label free technique.[27]

KD values determined are reported in Table 1. Among the conceived derivatives of compound **5a** (Ala—Gly—Pro—Phe) used as starting template, which provides a KD in the low micromolar range (~6 μM), compounds **5b** and **5h**, in which the Gly residue is replaced by a Val and a Ser respectively, possess a similar or a slightly increased binding affinity to Pin1 (Table 1). On the other hand, the introduction of long-side chain residues, such as Arg (**5d**), Glu (**5e**), Lys (**5j**), Met (**5l**), Gln (**5m**), Orn (**5o–n**) decreased the binding affinity of the resulting derivatives for Pin1, indicating that the affinity is reduced as the steric hindrance of the residues increases. In line with this evidence, compounds **5c**, **5e**, **5f**, **5g** and **5i** show a very little or no binding affinity to Pin1. However, the replacement of Gly in **5a** with His in **5k**, provides a significant increase of the binding

affinity to Pin1. Indeed, the affinity of **5k** toward Pin1 is in the range of 0.45 μM, which is about 10-fold tighter than the affinity of **5a** toward the same protein (6.09 μM) (Table 1), suggesting that the imidazole ring can stabilize the complex by additional interactions. The presence of D—Pro into compound **5p**, analogous of **5j**, abrogates the interaction with Pin1.

Peptides **5e**, **5i** and **5k** bind to Pin4, in a dose-dependent manner, reaching the steady state and showing KDs in the micromolar range (Table 1). Comparing the KD values obtained for Pin1 and Pin4, it seems that Pin4 better allocates bulky residues before the Pro than Pin1. Indeed, compounds **5e** and **5i** bind Pin4 better than Pin1. Compound **5k** efficiently binds Pin4, while showing a KD of about 12-fold lower for Pin4 with respect to Pin1, suggesting a lower contribution of the imidazole ring in stabilizing the complex.

ChemMedChem

Research Article
doi.org/10.1002/cmdc.202200050

Chemistry
Europe
European Chemical
Societies Publishing

Molecular modeling studies

Among the conceived compounds, 5k showed the highest affinity against Pin1, leading to the most promising compound of the series. Molecular modeling studies highlighted the different interactions in Pin1 and Pin4 binding sites. As expected, 5k is able to perfectly accommodate the Pro residue into the catalytic cleft formed by the catalytic tetrad (Figure 3, H59, H157, C113, and T152 in Pin1; H42, H123, D74, and T118 in Pin4) in both enzymes. Regarding Pin1 enzyme, the binding analysis revealed that compound 5k showed a stronger pattern of interaction compared to Pin4. In fact, 5k in Pin1 strongly targeted the Arg-rich region (R68 and R69) belonging to the long loop between β1 and α1 motif that is absent in Pin4 (Figure 3A). Moreover, His residues of 5k established H-bonds with the backbone of Q129 and the sidechain of Q131. The Phe residue is accommodated in a hydrophobic sub-pocket composed of L122, F125, and M130 (Figure 3A). As for the Pin4 enzyme, compound 5k established limited contacts within the binding site. In fact, we observed only H-bonds with the side chain of K75 and the backbone of S89. Hydrophobic interactions were observed between the Phe of 5k and residues M85 and M90 of Pin4 (Figure 3B). Accordingly, due to the absence of the mentioned loop in Pin4, compound 5k lacks relevant affinity for this enzyme, as highlighted by in silico investigation. Furthermore, the different pattern of interactions with the enzymes, combined with the docking score evaluation (5k into Pin1-7.665 kcal/mol; 5k into Pin4-4.417 kcal/mol), strongly supports the experimentally determined different affinity against the two enzymes (see Table 1).

Investigation of 5a–p activity in cell-based assays and preparation of R8 conjugated peptides

Oligopeptides 5d, 5f–k, structurally and chemically diversified among them, were tested in cancer cell lines to evaluate the potential anti-proliferative activity. As shown in Figure 4, no significant effects were registered in cells treated with compounds at 100 μM compared to the untreated cells, used as control, likely because of their poor cell permeability (Figure 4). Therefore, the best compounds 5k and 5i (which bind both Parvulins) were chosen for a more in-depth analysis, while the well-known polyarginine-based sequence (octaarginine, R8) as CPP. The R8 stretch was added at N-terminus and each peptide was synthesized through the Fmoc-based solid phase method-
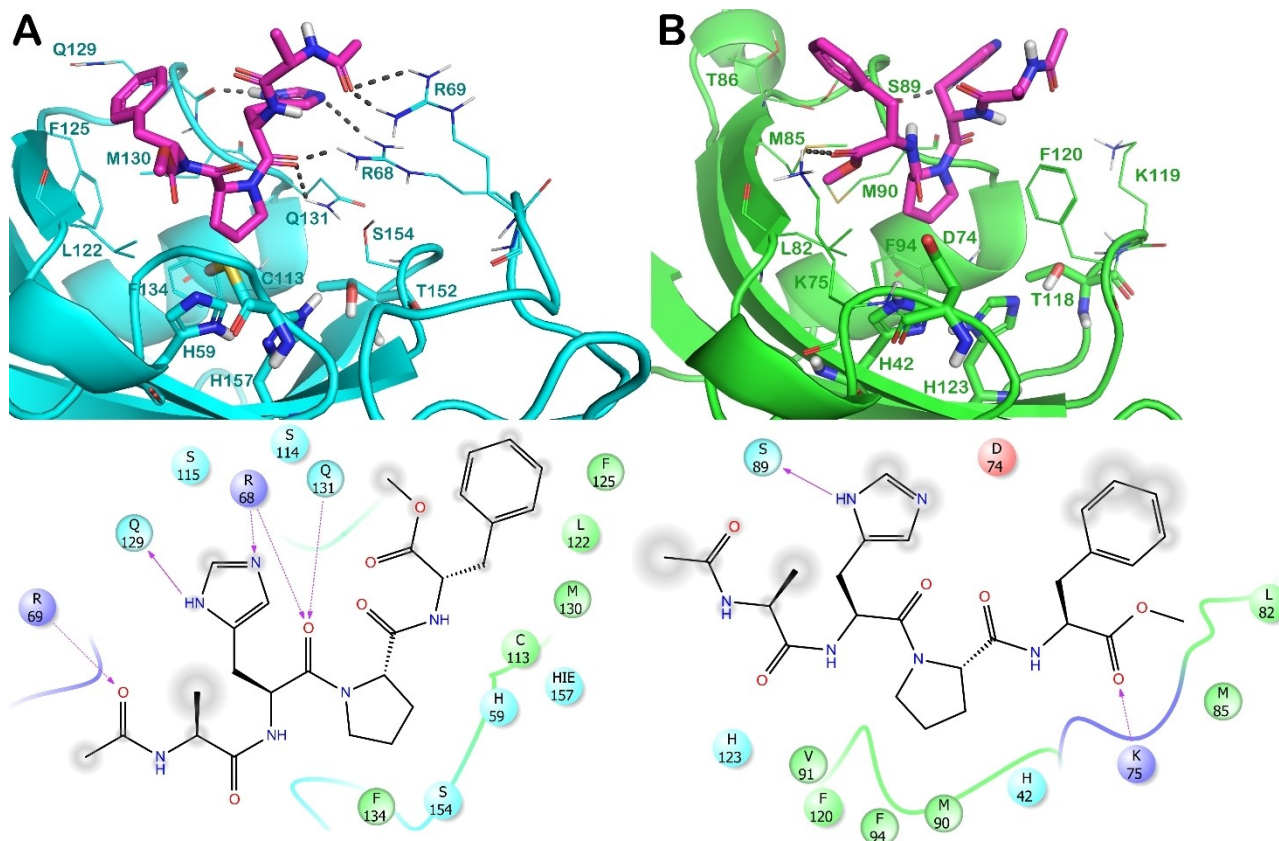
Figure 3. Docked poses of compound 5k (magenta sticks) within Pin1 (cyan cartoon, panel A) and Pin4 (green cartoon, panel B). Interacting residues in binding sites are represented by lines and the catalytic tetrads by sticks (H59, H157, C113, and T152 in Pin1; H42, H123, D74, and T118 in Pin4). For the sake of clarity, H157 in Pin1 was reported as HIE157 (HIE stands for tautomeric histidine) in the ligand interaction diagram according to the protein preparation output. H-bonds are illustrated by grey dotted lines. Pictures were generated by PyMOL (The PyMOL Molecular Graphics System, v1.8; Schrödinger, LLC, New York, 2015) and by Ligand interaction diagram available in Maestro.

ChemMedChem

Research Article
doi.org/10.1002/cmdc.202200050

**Chemistry
Europe**
European Chemical
Societies Publishing

Figure 4. A549, HCT116 and MCF7 were treated with selected oligopeptides without R8 (100 μM) and cell viability was detected by MTT assay. Results are presented as percentage of vitality of control (untreated cells) and represent mean ± S.D. of three independent experiments.

ology (see Materials and Methods for details). LC-MS analysis confirmed the identity of peptides (Figure S1).
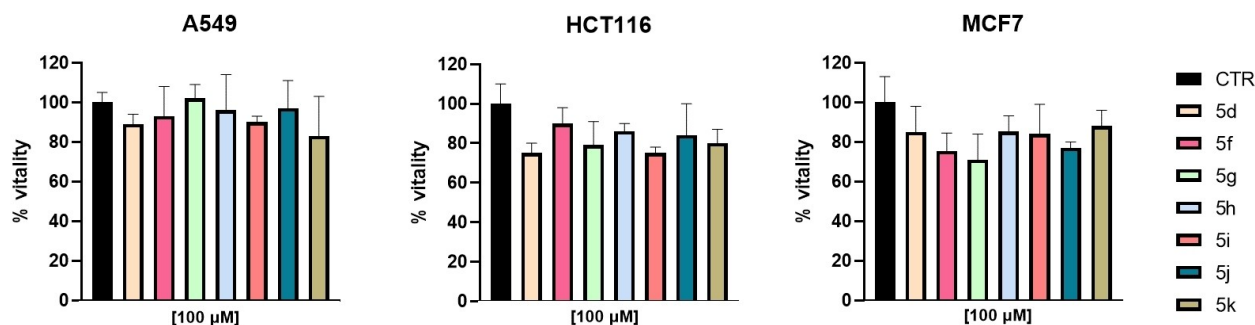
Investigation of R8–5i and R8–5k activity in vitro and in cell-based assays

To assess the effects of R8 stretch on the affinity of peptides toward Pin enzymes, direct binding assays were carried out (Figure 5). Noteworthy, the addition of a polyarginine tail at *N*-terminus significantly increased the affinity of peptides to Pin4, whereas negligible effects were observed for Pin1. In particular, testing the peptides at low concentrations (from 0 to 2.0 μM) against Pin1, we found that **R8–5i** does not reach saturation, preventing an accurate determination of KD in these experimental conditions, in agreement with a KD of about 70 μM determined for the parent compound (**5i**). On the contrary, the peptide **R8–5k** binds Pin1 in a concentration-dependent and saturable manner, showing a KD value of 0.13 ± 0.02 μM, in line with the KD determined for **5k** to Pin1 (see Table 1). Notably, the R8 conjugated peptides bind Pin4 with a higher affinity than unconjugated compounds, showing KD values of 0.56 ± 0.02 μM and 0.22 ± 0.05 μM for **R8–5i** and **R8–5k**, respectively,

suggesting that the arginines may participate in the stabilization of the complex by forming additional interactions. However, the R8 tag, used as control in the binding assays, does not bind both Parvulins, in the range of concentrations tested. All together, these results suggested that the driving force of the interaction is mediated by the specific peptide sequence, and for Pin4, the positioning of the peptide in the catalytic pocket could allow the arginine tail to stabilize the complex with further interactions. The two peptides (**R8–5i** and **R8–5k**) were also tested for the anti-proliferative activity against different cancer cell lines, where Pin proteins are over-expressed, using 3-(4,5-dimethyl thiazole-2-yl)-2,5-diphenyl tetrazolium bromide (MTT) cell assay. This preliminary analysis showed that these peptides reduced the cell proliferation of about 50–60%, in all cancer cells tested, already after 24 h of induction at 10 μM concentration and the effect persisted up to 48 h (Figure 6 A–C). In contrast, a non-significant anti-proliferative activity, less than 20%, was evidenced in AC16 non-tumor system (Figure 6E). Similar results were also detected in PNT2 cell line that constitutes the normal prostate epithelium immortalized with SV40 model (Figure 6F).

The effect of the R8 tag was also tested to evaluate if the biological activity observed for the compounds tested could be
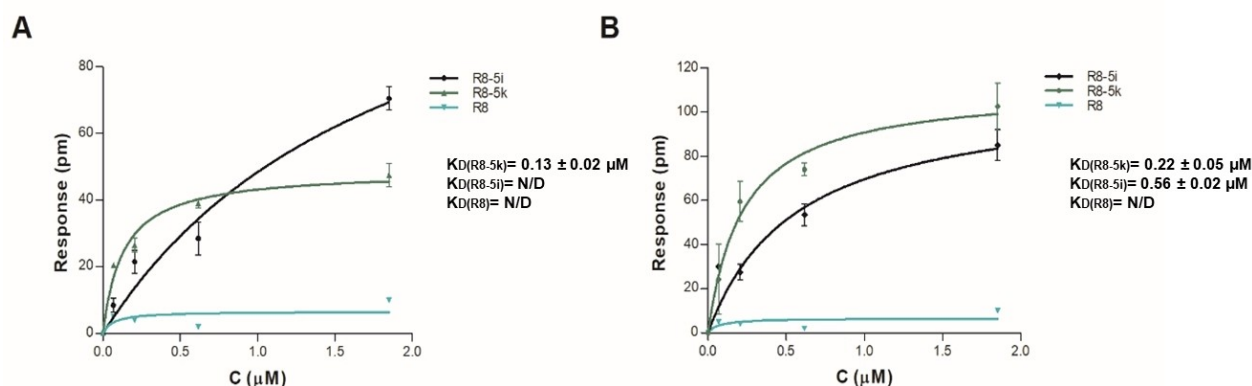

Figure 5. Binding curves of **R8–5i**, **R8–5k** and **R8** compounds against Pin1 (A) and Pin4 (B) proteins. Experiments were carried out using the Label-free Corning® Epic® technology. N/D: KDs not determined or could not be accurately determined in the concentration range used in the assays.
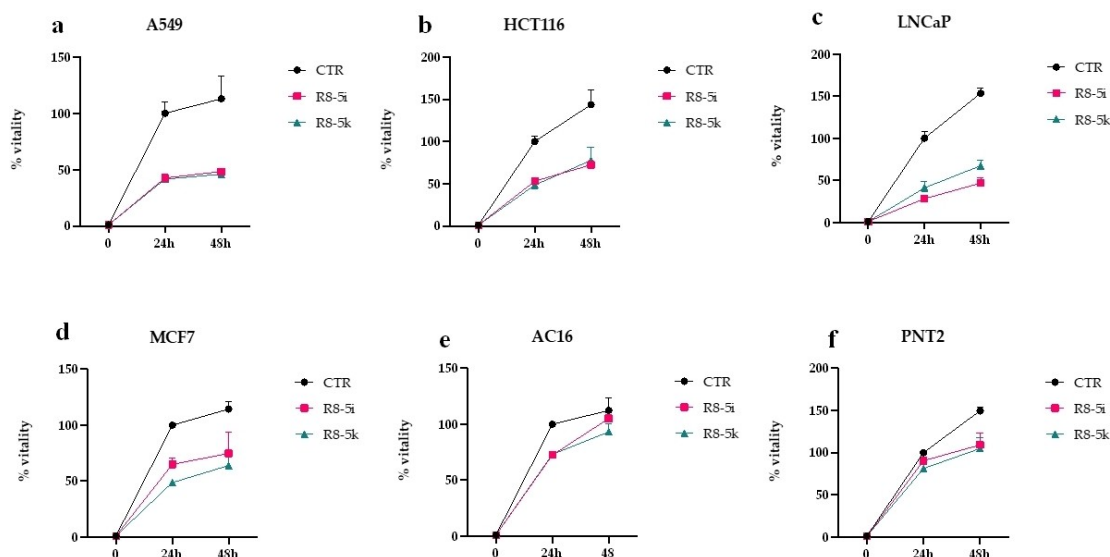
ChemMedChem

Research Article
doi.org/10.1002/cmdc.202200050

Chemistry Europe
European Chemical
Societies Publishing

Figure 6. Different cell lines were treated with oligopeptides conjugated with a poly-arginine stretch (10 μM) for 24 h and 48 h and cell viability was measured by MTT assay. Results are presented as percentage of vitality of control (untreated cells), and represent mean ± S.D. of three independent experiments.

ascribed to the R8 alone. R8, tested at 10 μM, reduced the cell proliferation of about 20–30% on HCT116 cells treated for 24 h (Figure 7), which is much less than that observed upon **R8**–**5i** and **R8**–**5k** treatment (~60%) in the same experimental conditions. These data demonstrated how the observed antiproliferative effect of **R8**–**5i,k** is also due to the presence of R8 stretch. Despite the literature claims about the R8 tag,[20,23,24] these data confirm that R8 tag may not be appropriate to improve cell permeability of antiproliferative agents since it is not totally inert. A further evaluation of the biological effect of R8 conjugated oligopeptides and R8 alone was performed by a cytofluorimetric analysis in HCT116 cells. HCT116 cells were treated with **R8**–**5i**, **R8**–**5k** and **R8** alone at 10 μM. As shown in
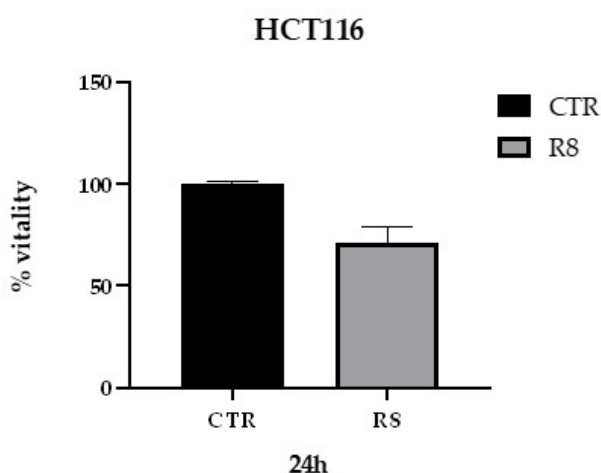

Figure 7. HCT116 cells were treated with R8 (10 μM) for 24 h and cell viability was detected by MTT assay. MTT results are presented as percentage of vitality of control (untreated cells), and represent mean ± S.D. of three independent experiments.

Figure 8, in agreement with MTT assays, oligopeptides block cell proliferation by stopping cells in G1 phase. Indeed, we observed a slight increase of cells within G1 phase when HCT116 cells were treated with **R8**–**5i** and **R8**–**5k** (66.4% and 61.2%, respectively) compared to control and R8 treated cells (about 50.5% and 57.4%, respectively) after 48 h (Figure 8).

Conclusion

By combining molecular modelling, chemical synthesis and biological investigation, we discovered new peptide-based Pin1 inhibitors. Sixteen new compounds were synthesized and tested against Pin1 and Pin4 through direct-binding assays. Compounds **5b**, **5h**, **5k**, and **5l** showed high Pin1 inhibitory activity, and compounds **5g** and **5k** displayed significant binding to Pin4. In particular, the oligopeptide **5k** showed an inhibitory potency of Pin1 in the high nanomolar range, whereas a lower affinity was determined for Pin4 (12-fold). Docking studies revealed significant interaction between **5k** and Pin1 active site and highlighted the differences in the binding mode of the selected compound, against both Pin1 and Pin4. Since the molecule did not show antiproliferative activity, probably due to low cell penetration as demonstrated for other peptide molecules, to evaluate the effects of peptide **5k** in cancer cells, cell permeability of compounds **5k** was attained by R8 conjugation. Conjugation of the peptides with an arginine tail at the *N*-terminus significantly reduced their selectivity toward Pin1 and Pin4. When tested on cancer cell lines, **R8**–**5k** showed an encouraging anti-proliferative effect after 24 h of treatment that lasts up to 48 h, without any notable effect on non-cancer cells. However, we found out that the R8 fragment was responsible, at least in part, of the antiproliferative effect of **R8**–**5k** and **R8**–**5i**, indicating that R8 is

ChemMedChem

Research Article
doi.org/10.1002/cmdc.202200050

**Chemistry
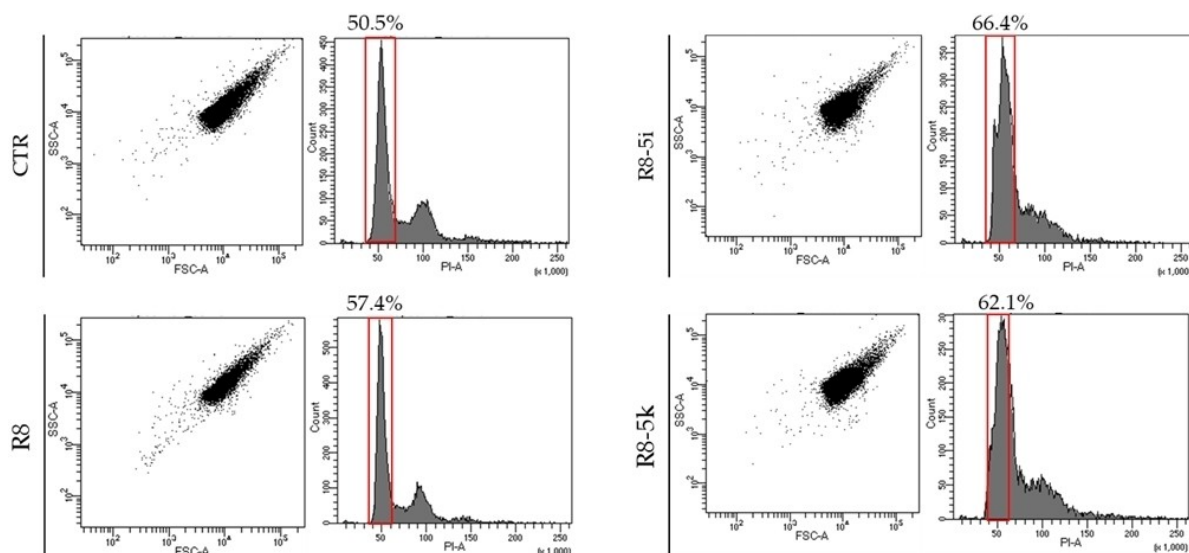Europe**
European Chemical
Societies Publishing

Figure 8. Representative graphs of cell cycle distribution. HCT116 cells were treated with oligopeptides at 10 μM for 48 h. Cells were evaluated as SSC-A/FSC-A and for PI-A intensity.

not the most appropriate tool for improving cell permeability of antiproliferative peptides in our experimental conditions. Further research efforts are ongoing aiming at improving cell penetration and antiproliferative action of our peptide-based Parvulin inhibitors.

Experimental Section

General chemical information

Unless otherwise specified, materials were purchased from commercial suppliers and used without further purification. Reaction progress was monitored by TLC using silica gel 60 F254 (0.040–0.063 mm) with detection by UV. Silica gel 60 (0.040–0.063 mm) or aluminum oxide 90 (0.063–0.200 mm) were used for column chromatography. ^{1}H NMR, and ^{13}C NMR spectra were recorded on a Varian 300 MHz, spectrometer by using the residual signal of the deuterated solvent as internal standard. Splitting patterns are described as singlet (s), doublet (d), triplet (t), quartet (q), quintet (p), and broad (br); the value of chemical shifts (d) are given in ppm and coupling constants (*J*) in Hertz (Hz). ESI-MS spectra were performed by an Agilent 1100 Series LC/MSD spectrometer. Yields refer to purified products and are not optimized. All moisture-sensitive reactions were performed under argon atmosphere using oven-dried glassware and anhydrous solvents.

Methyl L-prolyl-L-phenylalaninate (6). According with published procedure, compound **6** was obtained as a colorless oil.[25]

Acetyl-L-alanine (8). According with published procedure compound **8** was obtained as a colorless oil.[26]

General procedure i) To a solution of the corresponding carboxylic acid (1 eq, 0.04 mmol) in dry DCM (5 mL) at 0 °C, EDCI (1.2 eq, 0.048 mmol), HOBt (1.5 eq, 0.06 mmol) and DIPEA (4 eq, 0.16 mmol) were added. After 10 min, the corresponding amine (1.2 eq, 0.048) was added. The mixture was allowed to warm room temperature and stirred for 12 h. Solvent was removed and the pure compound

was obtained after flash chromatography by using a gradient of *n*-hexane:EtOAc from 90:10 to 50:50.

Methyl (tert-butoxycarbonyl)glycyl-L-prolyl-L-phenylalaninate (7a). The title compound was obtained according with general procedure i) by reacting **6** with Boc-Gly-OH. Colorless oil, 87% yield. ^{1}H NMR (300 MHz, CDCl$_3$) δ 7.44–6.91 (m, 5H), 5.36 (s, 1H), 4.77 (m, 1H), 4.57–4.39 (m, 1H), 4.05 (q, *J*=7.1 Hz, 1H), 3.89–3.73 (m, 1H), 3.73–3.51 (m, 3H), 3.31–3.05 (m, 2H), 2.98–2.79 (m, 1H), 2.39–2.16 (m, 1H), 1.97 (s, 2H), 1.91–1.77 (m, 1H), 1.77–1.61 (m, 1H), 1.39 (d, *J*=10.7 Hz, 6H), 1.26–1.04 (m, 2H). ESI-MS: 456 [M+Na]$^+$

Methyl (tert-butoxycarbonyl)-L-valyl-L-prolyl-L-phenylalaninate (7b). The title compound was obtained according with general procedure i) by reacting **6** with Boc-Val-OH. Colorless oil, 56% yield. ^{1}H NMR (300 MHz, CDCl$_3$) δ 7.43–6.83 (m, 6H), 5.23 (d, *J*=9.3 Hz, 1H), 4.74 (m, 1H), 4.53 (m, 1H), 4.22 (m, 1H), 3.81–3.53 (m, 4H), 3.46 (m, 1H), 3.17–2.94 (m, 2H), 2.41–2.12 (m, 1H), 2.06–1.68 (m, 4H), 1.40 (m, 9H), 1.01–0.69 (m, 6H). ESI-MS: 476 [M+Na]$^+$

Methyl N^2-(((9H-fluoren-9-yl)methoxy)carbonyl)-N^ω-((4-methoxy-2,3,6-trimethylphenyl)sulfonyl)-L-arginyl-L-prolyl-D-phenylalaninate (7c). The title compound was obtained according with general procedure i) by reacting **6** with Fmoc-Arg(Mtr)-OH. White solid, 32% yield. ^{1}H NMR (300 MHz, CDCl$_3$) δ 7.72 (d, *J*=7.5 Hz, 2H), 7.55 (d, *J*=7.3 Hz, 2H), 7.41–6.98 (m, 10H), 6.77 (d, *J*=7.3 Hz, 1H), 6.48 (s, 1H), 6.25 (m, 2H), 5.89 (m, 1H), 5.34–5.21 (m, 1H), 4.81–4.56 (m, 1H), 4.53–4.04 (m, 5H), 3.85–3.29 (m, 8H), 3.27–2.81 (m, 3H), 2.76–2.45 (m, 8H), 2.22–0.94 (m, 9H). ESI-MS: 890 [M+Na]$^+$.

tert-Butyl (S)-4-((((9H-fluoren-9-yl)methoxy)carbonyl)amino)-5-((S)-2-(((R)-1-methoxy-1-oxo-3-phenylpropan-2-yl)carbamoyl)pyrrolidin-1-yl)-5-oxopentanoate (7e). The title compound was obtained according with general procedure i) by reacting **6** with Fmoc-Glu(OtBu)-OH. White solid, 25% yield. ^{1}H NMR (300 MHz, CDCl$_3$) δ 7.83–7.69 (m, 2H), 7.57 (dd, *J*=7.5, 4.3 Hz, 2H), 7.44–6.99 (m, 9H), 5.65 (d, *J*=8.7 Hz, 1H), 4.80 (q, *J*=6.6 Hz, 1H), 4.67–4.47 (m, 2H), 4.40–4.26 (m, 2H), 4.18 (t, *J*=7.0 Hz, 3H), 3.69 (s, 3H), 3.67–3.57 (m, 2H), 3.23–2.94 (m, 2H), 2.42–2.15 (m, 3H), 1.99–1.77 (m, 4H), 1.44 (s, 9H). ESI-MS: 706 [M+Na]$^+$.

Methyl O-benzyl-N-(tert-butoxycarbonyl)-L-seryl-L-prolyl-L-phenylalaninate (7g). The title compound was obtained according with general

ChemMedChem

Research Article
doi.org/10.1002/cmdc.202200050

**Chemistry
Europe**

European Chemical
Societies Publishing

procedure i) by reacting **6** with Boc-Ser(OBn)-OH. White solid, 50% yield. ^{1}H NMR (300 MHz, CDCl$_3$) δ 7.71 (m, 1H), 7.36–6.80 (m, 10H), 6.48 (d, J=7.4 Hz, 1H), 5.24 (s, 1H), 5.01–4.99 (m, 1H), 4.74–4.47 (m, 3H), 4.44–4.19 (m, 2H), 3.82–3.40 (m, 7H), 3.00–2.62 (m, 2H), 2.17–1.69 (m, 7H), 1.27–1.24 (m, 4H). ESI-MS: 576 [M+Na]$^+$.

Methyl N^6-((benzyloxy)carbonyl)-N^2-(tert-butoxycarbonyl)-L-lysyl-L-prolyl-D-phenylalaninate (7i). The title compound was obtained according with general procedure i) by reacting **6** with Boc-Lys(Cbz)-OH. Colorless oil, 83% yield. ^{1}H NMR (400 MHz, CDCl$_3$) δ 7.51–6.99 (m, 8H), 6.70 (d, J=7.3 Hz, 2H), 5.25 (d, J=8.7 Hz, 1H), 5.20–4.96 (m, 3H), 4.77 (q, J=6.1 Hz, 1H), 4.60–4.30 (m, 2H), 3.81–3.54 (m, 4H), 3.53–3.38 (m, 1H), 3.28–2.98 (m, 4H), 2.32–2.10 (m, 1H), 2.04–1.85 (m, 2H), 1.52 (s, 8H), 1.41 (s, 9H). ESI-MS: 661 [M+Na]$^+$.

Methyl N^α-(((9H-fluoren-9-yl)methoxy)carbonyl)-N^τ-trityl-L-histidyl-L-prolyl-L-phenylalaninate (7k). The title compound was obtained according with general procedure i) by reacting **6** with Fmoc-His(Trt)-OH. White solid, 86% yield. ^{1}H NMR (300 MHz, CDCl$_3$) δ 9.21 (d, J=8.4 Hz, 1H), 7.85–7.43 (m, 4H), 7.45–6.93 (m, 22H), 6.70 (d, J=10.4 Hz, 1H), 6.05–5.83 (m, J=10.7 Hz, 1H), 5.07–4.80 (m, 1H), 4.77–4.43 (m, 2H), 4.41–3.93 (m, 3H), 3.50 (d, J=17.1 Hz, 3H), 3.42–3.07 (m, 2H), 3.15–2.79 (m, 5H), 2.54 (s, 1H), 2.24–1.88 (m, 3H), 1.90–1.52 (m, 2H). ESI-MS: 879 [M+H]$^+$.

Methyl ((benzyloxy)carbonyl)-L-methionyl-L-prolyl-L-phenylalaninate (7l). The title compound was obtained according with general procedure i) by reacting **6** with Cbz-Met-OH. White amorphous solid, 47% yield. ^{1}H NMR (300 MHz, CDCl$_3$) δ 7.46–6.87 (m, 10H), 5.51–5.29 (m, 3H), 5.02 (d, J=14.2 Hz, 2H), 4.40 (s, 1H), 4.01 (s, 1H), 3.83–3.66 (m, 3H), 3.20 (d, J=36.4 Hz, 2H), 2.87 (s, 1H), 2.76–2.60 (m, 2H), 2.54–2.42 (m, 3H), 2.38 (s, 1H), 2.24 (d, J=16.9 Hz, 2H), 2.06 (t, J=22.5 Hz, 3H). ESI-MS: 542 [M+H]$^+$.

Methyl N^2-(((9H-fluoren-9-yl)methoxy)carbonyl)-N^5-trityl-L-glutaminyl-L-prolyl-L-phenylalaninate (7m). The title compound was obtained according with general procedure i) by reacting **6** with Fmoc-Gln(Trt)-OH. White oil, 60% yield. ^{1}H NMR (300 MHz, CDCl$_3$) δ 7.75 (d, J=7.4 Hz, 2H), 7.64–7.46 (m, 2H), 7.44–6.88 (m, 24H), 5.51 (d, J=8.6 Hz, 2H), 5.29 (d, J=0.4 Hz, 2H), 4.83–4.66 (m, 2H), 4.54–4.00 (m, 5H), 3.68 (s, 2H), 3.22–2.96 (m, 2H), 2.93–2.79 (m, 1H), 2.52–2.16 (m, 1H), 2.13–1.32 (m, 6H), 1.31–1.09 (m, 1H). ESI-MS: 870 [M+H]$^+$.

Methyl (5-(((benzyloxy)carbonyl)amino)-2-((tert-butoxycarbonyl)amino)pentanoyl)-L-prolyl-L-phenylalaninate (7n). The title compound was obtained according with general procedure i) by reacting **6** with Boc-Orn(Cbz)-OH. Colorless oil, 83% yield. ^{1}H NMR (400 MHz, CDCl$_3$) δ 7.59–6.95 (m, 10H), 6.70 (d, J=6.6 Hz, 1H), 5.39–4.95 (m, 4H), 4.91–4.62 (m, 1H), 4.64–4.32 (m, 2H), 3.64 (dd, J=19.1, 8.4 Hz, 5H), 3.44 (d, J=4.4 Hz, 1H), 3.35–2.88 (m, 5H), 2.51–1.76 (m, 6H), 1.78–0.98 (m, 9H).

tert-Butyl 2-(((S)-1-methoxy-1-oxo-3-phenylpropan-2-yl)carbamoyl)pyrrolidine-1-carboxylate (12). Starting from **11**, the title compound was obtained according with general procedure i). White solid, 98% yield. ^{1}H NMR (300 MHz, CDCl$_3$) δ 7.36–6.94 (m, 5H), 4.79 (s, 1H), 4.38–3.99 (m, 1H), 3.62 (s, 3H), 3.47–3.12 (m, 2H), 3.04 (d, J=6.0 Hz, 2H), 2.36–1.58 (m, 5H), 1.59–1.18 (m, 9H).

Procedures for Boc and Fmoc deprotection

General procedure ii for Boc deprotection: To a solution of the Boc-protected amino acid (1 eq, 0.04 mmol) in dry DCM (10 mL) at 0 °C, 10% TFA was added dropwise. The mixture was stirred at 0 °C for 1 h. Then, it was diluted with DCM (5 mL) and a saturated aqueous solution of NaHCO$_3$ was added until neutralization. The mixture was partitioned between water and DCM; the organic layer was dried with Na$_2$SO$_4$, filtered, and evaporated *in vacuo*. The crude product was used without further purification.

General procedure iii for Fmoc deprotection: To a stirred solution of Fmoc-protected amino acid (1 eq, 0.1 mmol) in DCM (10 mL), a 20% solution of piperidine in DCM was added and the mixture stirred for 3 h at room temperature. The solvent was removed, the residue was washed multiple times by a co-evaporation with DCM (3×20 mL), to obtain the pure compound; if not pure, the crude residue was further purified through flash chromatography by using DCM/MeOH (20:1 v/v) as eluent.

Methyl glycyl-L-prolyl-L-phenylalaninate (8a). Starting from **7a**, the title compound was obtained according with general procedure ii). Colorless oil, 75% yield. ^{1}H NMR (300 MHz, CDCl$_3$) δ 7.40 (d, J=7.5 Hz, 1H), 7.29–6.84 (m, 6H), 4.91–4.64 (m, 1H), 4.50 (d, J=6.9 Hz, 1H), 3.80–3.52 (m, 3H), 3.49–2.70 (m, 4H), 2.40–2.15 (m, 1H), 2.10–1.41 (m, 5H), 1.30–1.07 (m, 1H). ESI-MS: 334 [M+H]$^+$.

Methyl L-valyl-L-prolyl-L-phenylalaninate (8b). Starting from **7b**, the title compound was obtained according with general procedure ii). Colorless oil, 76% yield. ^{1}H NMR (300 MHz, CDCl$_3$) δ 7.39–6.84 (m, 7H), 4.93–4.63 (m, 1H), 4.64–4.47 (m, 1H), 3.68 (m, 1H), 3.64 (s, 3H), 3.57–3.34 (m, 2H), 3.34–2.80 (m, 2H), 2.36–2.19 (m, 2H), 2.15–1.56 (m, 2H), 1.44–1.08 (m, 2H), 1.08–0.66 (m, 6H).

Methyl N^ω-((4-methoxy-2,3,6-trimethylphenyl)sulfonyl)-L-arginyl-L-prolyl-L-phenylalaninate (8c). Starting from **7c**, the title compound was obtained according with general procedure iii). Colorless oil, 100% yield. ^{1}H NMR (300 MHz, CDCl$_3$) δ 7.32–6.85 (m, 5H), 6.44 (d, J=20.1 Hz, 3H), 4.84–4.54 (m, 1H), 4.46–4.43 (m, 1H), 3.89–3.51 (m, 6H), 3.56–3.30 (m, 2H), 3.28–2.81 (m, 2H), 2.77–2.36 (m, 5H), 2.31–1.70 (m, 6H), 1.74–1.06 (m, 5H). ESI-MS: 667 [M+H]$^+$.

tert-Butyl (S)-4-amino-5-((S)-2-(((R)-1-methoxy-1-oxo-3-phenylpropan-2-yl)carbamoyl)pyrrolidin-1-yl)-5-oxopentanoate (8e). Starting from **7e**, the title compound was obtained according with general procedure iii). Purification by column chromatography (DCM/MeOH (20:1 v/v) furnished the title compound. Colorless oil, 85% yield. ^{1}H NMR (300 MHz, CDCl$_3$) δ 7.34–7.02 (m, 5H), 4.90–4.75 (m, 1H), 4.58–4.40 (m, 1H), 3.70 (s, 3H), 3.28–2.88 (m, 2H), 2.53–2.18 (m, 8H), 2.16–1.72 (m, 6H), 1.42 (s, 9H). ESI-MS: 462 [M+H]$^+$.

Methyl O-benzyl-L-seryl-L-prolyl-L-phenylalaninate (8g). Starting from **7g**, the title compound was obtained according with general procedure ii). Colorless oil, 49% yield. ^{1}H NMR (300 MHz, CDCl$_3$) δ 7.30– 7.10 (m, 10H), 6.48 (d, J=7.4 Hz, 1H), 5.24 (s, 1H), 5.01- 4.99 (m, 1H), 4.74–4.47 (m, 2H), 4.44–4.19 (m, 2H), 3.82–3.40 (m, 5H), 3.00–2.62 (m, 2H), 2.17–1.69 (m, 4H), 1.27–1.24 (m, 3H). ESI-MS: 454 [M+H]$^+$.

Methyl N^6-((benzyloxy)carbonyl)-L-lysyl-L-prolyl-L-phenylalaninate (8i). Starting from **7i**, the title compound was obtained according with general procedure ii). Colorless oil, 64% yield. ^{1}H NMR (400 MHz, CDCl$_3$) δ 7.40–7.04 (m, 10H), 6.96 (s, 1H), 5.41 (s, 1H), 5.05 (d, J=4.4 Hz, 2H), 4.94–4.64 (m, 1H), 4.52 (s, 1H), 3.71 (d, J=11.6 Hz, 1H), 3.65 (s, 3H), 3.40 (t, J=31.4 Hz, 2H), 3.26–2.95 (m, 6H), 2.21–2.07 (m, 2H), 1.95–1.87 (m, 4H), 1.72–1.39 (m, 4H).

Methyl N^τ-trityl-L-histidyl-L-prolyl-L-phenylalaninate (8k). Starting from **7i**, the title compound was obtained according with general procedure iii). Colorless oil, 100% yield. ^{1}H NMR (300 MHz, CDCl$_3$) δ 8.59 (d, J=8.1 Hz, 1H), 7.44–6.87 (m, 21H), 6.61 (dd, J=16.5, 1.1 Hz, 1H), 4.85–4.80 (m, 1H), 4.68–4.52 (m, 1H), 3.83–3.57 (m, 2H), 3.53 (s, 3H), 3.45–3.23 (m, 1H), 3.24–2.54 (m, 4H), 2.48–1.90 (m, 4H), 1.86–1.57 (m, 1H), 1.55–1.23 (m, 1H).

Methyl L-methionyl-L-prolyl-L-phenylalaninate (8l). Starting from **7l**, the title compound was obtained according with general procedure ii). White amorphous solid, 92% yield. ^{1}H NMR (300 MHz, CDCl$_3$) δ

ChemMedChem

Research Article
doi.org/10.1002/cmdc.202200050

Chemistry
Europe
European Chemical
Societies Publishing

7.35–7.02 (m, 5H), 6.80 (s, 1H), 4.77 (s, 1H), 4.40 (s, 1H), 4.00 (d, $J=$ 12.8 Hz, 2H), 3.73–3.58 (m, 3H), 3.41 (d, $J=33.0$ Hz, 2H), 3.10 (s, 1H), 2.86–2.63 (m, 2H), 2.49–2.26 (m, 4H), 2.26–1.93 (m, 5H), 1.84 (s, 1H), 1.71 (s, 1H). ESI-MS: 429 [M + Na]$^+$.

Methyl N^5-trityl-L-glutaminyl-L-prolyl-L-phenylalaninate (8 m). Starting from **7 m**, the title compound was obtained according with general procedure iii). Purification by column chromatography (DCM/MeOH (20:1 v/v) furnished the title compound. White amorphous solid, 89% yield. ^{1}H NMR (300 MHz, CDCl$_3$) δ 7.43–7.05 (m, 20H), 7.00–6.87 (m, 2H), 4.85–4.65 (m, 1H), 4.42 (dd, $J=8.1$, 3.3 Hz, 1H), 3.64 (s, 3H), 3.20–2.90 (m, 4H), 2.89–2.70 (m, 1H), 2.64–2.41 (m, 1H), 2.35–2.20 (m, 1H), 1.94 (s, 4H), 1.89–1.67 (m, 2H), 1.66–1.44 (m, 2H).

Methyl ((S)-2-amino-5-(((benzyloxy)carbonyl)amino)pentanoyl)-L-prolyl-L-phenylalaninate (8 n). Starting from **7 n**, the title compound was obtained according with general procedure ii). White amorphous solid, 98% yield. ^{1}H NMR (400 MHz, CDCl$_3$) δ 7.61–6.61 (m, 10H), 5.34 (d, $J=49.8$ Hz, 1H), 5.03 (d, $J=15.9$ Hz, 2H), 4.93–4.05 (m, 3H), 3.95–2.42 (m, 10H), 2.35–0.93 (m, 10H).

Methyl N^α-(acetyl-L-alanyl)-N^τ-trityl-L-histidyl-L-prolyl-L-phenylalaninate (10 k). The title compound was obtained by reacting **8 k** and **9** according with general procedure i). Colorless oil, 100% yield. ^{1}H NMR (300 MHz, CDCl$_3$) δ 9.09 (d, $J=8.4$ Hz, 1H), 7.50–6.79 (m, 18H), 6.80–6.50 (m, 1H), 6.39 (dd, $J=21.2$, 7.4 Hz, 1H), 4.98–4.73 (m, 1H), 4.74–4.43 (m, 2H), 4.40–4.11 (m, 1H), 3.68–2.51 (m, 9H), 2.32–1.45 (m, 6H), 1.42–0.83 (m, 4H).

Methyl D-prolyl-L-phenylalaninate (13). According with general procedure ii), the title compound was obtained starting from **12**. ^{1}H NMR (300 MHz, CDCl$_3$) δ 8.17–7.90 (m, 2H), 7.38–7.04 (m, 5H), 5.36–5.20 (m, 1H), 4.88–4.71 (m, 1H), 4.67 (s, 1H), 3.80 (s, 3H), 3.31–2.72 (m, 3H), 2.27–1.52 (m, 4H).

Methyl N^2-(acetyl-L-alanyl)-N^6-((benzyloxy)carbonyl)-L-lysyl-D-prolyl-L-phenylalaninate (14). According with general procedure iii), the title compound was obtained was obtained from **13** coupled with N^2-(acetyl-L-alanyl)-N^6-((benzyloxy)carbonyl)-L-lysine, previously synthesized. ^{1}H NMR (300 MHz, CDCl$_3$) δ 8.32 (d, $J=8.4$ Hz, 1H), 7.71 (d, $J=7.1$ Hz, 1H), 7.50–6.97 (m, 10H), 6.62–6.53 (m, 1H), 5.91–5.82 (m, 1H), 5.20–4.52 (m, 6H), 3.89–3.42 (m, 5H), 3.20–2.70 (m, 4H), 2.35–1.71 (m, 8H), 1.76–0.93 (m, 8H).

Removal of Cbz protecting group

General procedure iv. A stirred solution of Cbz-protected amino acid (1 eq.) in MeOH (3 mL) was subjected to a hydrogen flux under Pd/C catalysis for 12 h. The mixture was filtered and pure compound used without further purification.

Methyl acetyl-L-alanylglycyl-L-prolyl-L-phenylalaninate (5 a). According with general procedure i) the title compound was obtained by reacting **8 a** with **9**. Colorless oil, 74% yield. ^{1}H NMR (300 MHz, CDCl$_3$) δ 7.55 (s, 1H), 7.41 (d, $J=7.8$ Hz, 1H), 7.30–6.99 (m, 5H), 6.84–6.53 (m, 1H), 4.95–4.40 (m, 2H), 4.11–3.72 (m, 2H), 3.60 (s, 3H), 3.52–3.23 (m, 3H), 3.21–2.80 (m, 3H), 2.45 (s, 1H), 2.24–1.64 (m, 5H), 1.52–1.05 (m, 3H). ^{13}C NMR (75 MHz, CDCl$_3$) δ 172.9, 172.1, 170.8, 170.1, 167.6, 136.2, 128.9, 128.5, 128.3, 126.8, 59.8, 53.1, 52.2, 48.4, 46.4, 42.1, 37.5, 28.2, 24.3, 23.1, 18.9. ESI-MS: 469 [M+Na]$^+$.

Methyl acetyl-L-alanyl-L-valyl-L-prolyl-L-phenylalaninate (5 b). According with general procedure i) the title compound was obtained by reacting **8 b** with **9**. Colorless oil, 93% yield. ^{1}H NMR (300 MHz, CDCl$_3$) δ 8.25 (d, $J=9.4$ Hz, 1H), 7.67 (t, $J=18.5$ Hz, 1H), 7.40–6.86 (m, 5H), 6.51 (t, $J=20.9$ Hz, 1H), 4.99–4.60 (m, 4H), 3.97–3.29 (m, 5H), 3.25–2.68 (m, 2H), 2.43–1.55 (m, 8H), 1.53–0.50 (m, 9H). ^{13}C NMR (75 MHz, CDCl$_3$) δ 172.4, 171.7, 171.5, 170.9, 169.9, 136.3,

128.9, 128.3, 126.7, 59.7, 55.4, 53.9, 51.9, 48.4, 38.1, 31.5, 29.2, 24.8, 23.2, 19.9, 19.3, 17.9. ESI-MS: 511 [M+Na]$^+$.

Methyl N^2-(acetyl-L-alanyl)-N^ω-((4-methoxy-2,3,6-trimethylphenyl)sulfonyl)-L-arginyl-L-prolyl-L-phenylalaninate (5 c). According with general procedure i) the title compound was obtained by reacting **8 c** with **9**. Colorless oil, 80% yield. ^{1}H NMR (300 MHz, CDCl$_3$) δ 8.12 (s, 1H), 7.66 (d, $J=41.5$ Hz, 1H), 7.39–6.85 (m, 5H), 6.74 (dd, $J=23.5$, 7.2 Hz, 1H), 6.64–6.16 (m, $J=30.8$ Hz, 3H), 5.30–5.20 (m, 1H), 4.96–4.26 (m, 4H), 3.80–3.36 (m, 7H), 3.32–2.77 (m, 4H), 2.83–2.35 (m, 6H), 2.36–1.82 (m, 8H), 1.86–0.93 (m, 7H). ^{13}C NMR (75 MHz, CDCl$_3$) δ 172.2, 172.1, 171.5, 170.7, 170.5, 158.4, 156.3, 138.6, 135.8, 128.8, 128.5, 127.0, 124.7, 111.6, 60.0, 55.4, 54.1, 53.4, 52.1, 49.9, 48.6, 47.7, 37.5, 29.3, 24.9, 24.1, 23.6, 23.2, 19.4, 18.3, 11.9. MS: 545 [M+H]$^+$.

Methyl acetyl-L-alanyl-L-arginyl-L-prolyl-L-phenylalaninate (5 d). Starting from **5 c**, the title compound was obtained according with general procedure ii). Pale yellow amorphous solid, 90% yield. ^{1}H NMR (300 MHz, CD$_3$OD) δ 7.30–7.20 (m, 5H), 4.70–4.15 (m, 5H), 3.86–3.67 (m, 1H), 3.56–2.88 (m, 11H), 2.38–1.46 (m, 11H), 1.45–0.87 (m, 6H). ^{13}C NMR (75 MHz, CD$_3$OD) δ 173.8, 172.9, 171.8, 170.6, 157.2, 136.52, 128.9, 128.1, 126.5, 65.5, 59.9, 54.2, 51.2, 50.5, 49.2, 46.7, 40.6, 36.8, 29.1, 27.9, 24.4, 24.2, 20.9, 16.3, 14.0. ESI-MS: 546 [M + H]$^+$.

tert-Butyl (S)-4-((S)-2-acetamidopropanamido)-5-((S)-2-(((R)-1-methoxy-1-oxo-3-phenylpropan-2-yl)carbamoyl)pyrrolidin-1-yl)-5-oxopentanoate (5 e). The title compound was obtained by reacting **8 e** and **9** according with general procedure i). White amorphous solid, 67% yield. ^{1}H NMR (300 MHz, CDCl$_3$) δ 7.75 (d, $J=8.6$ Hz, 1H), 7.37 (d, $J=7.4$ Hz, 1H), 7.29–7.01 (m, 5H), 6.44 (d, $J=7.5$ Hz, 1H), 4.94–4.79 (m, 1H), 4.78–4.47 (m, 4H), 3.87–3.64 (m, 1H), 3.62 (s, 3H), 3.02 (dd, $J=7.5$, 6.7 Hz, 2H), 2.34–2.13 (m, 4H), 2.12–1.93 (m, 2H), 1.90 (s, 3H), 1.77–1.57 (m, 2H), 1.39 (s, 9H).

(S)-4-((R)-2-Acetamidopropanamido)-5-((S)-2-(((S)-1-methoxy-1-oxo-3-phenylpropan-2-yl)carbamoyl)pyrrolidin-1-yl)-5-oxopentanoic acid (5 f). Starting from **5 e**, the title compound was obtained according with general procedure ii). White amorphous solid, 75% yield. ^{1}H NMR (300 MHz, CDCl$_3$) δ 8.00–7.49 (m, 1H), 7.38–6.90 (m, 3H), 6.90–6.64 (m, 1H), 5.38–5.20 (m, 1H), 5.09–4.34 (m, 3H), 3.82–3.43 (m, 3H), 3.02 (dd, $J=15.0$, 6.2 Hz, 1H), 2.58–2.18 (m, 2H), 2.20–1.47 (m, 6H), 1.50–0.46 (m, 13H). ESI-MS: 519 [M+H]$^+$.

Methyl N-(acetyl-L-alanyl)-O-benzyl-L-seryl-L-prolyl-L-phenylalaninate (5 g). Starting from **8 g** in presence of compound **9**, the title compound was obtained according with general procedure i). Colorless oil, 55% yield. ^{1}H NMR (300 MHz, CDCl$_3$) δ 7.80–7.54 (m, 1H), 7.41–6.79 (m, 10H), 6.43 (t, $J=18.9$ Hz, 1H), 5.15–4.85 (m, 1H), 4.80–4.15 (m, 5H), 3.85–3.37 (m, 7H), 3.07–2.57 (m, 2H), 2.17–1.58 (m, 7H), 1.48–0.89 (m, 3H). ^{13}C NMR (75 MHz, CDCl$_3$) δ 172.3, 171.6, 170.8, 169.8, 169.5, 137.5, 136.3, 129.1, 128.4, 128.3, 127.7, 127.3, 126.7, 73.1, 70.1, 60.1, 53.3, 52.0, 50.4, 48.6, 47.7, 37.7, 28.7, 24.4, 23.1, 19.2. ESI-MS: 567 [M+H]$^+$.

Methyl acetyl-L-alanyl-L-seryl-L-prolyl-L-phenylalaninate (5 h). Starting from **5 g**, the title compound was obtained according with general procedure v). Colorless oil, 72% yield. ^{1}H NMR (300 MHz, CDCl$_3$) δ 7.93 (d, $J=8.4$ Hz, 1H), 7.41 (d, $J=7.8$ Hz, 1H), 7.30–7.01 (m, 5H), 6.70 (d, $J=7.6$ Hz, 1H), 5.06–4.91 (m, 1H), 4.81–4.64 (m, 2H), 3.85–3.78 (m, 2H), 3.69–3.64 (m, 3H), 3.63 (s, 3H), 3.09–2.89 (m, 2H), 2.19–1.80 (m, 5H), 1.32 (d, $J=7.0$ Hz, 1H), 1.23 (d, $J=6.8$ Hz, 2H). ^{13}C NMR (75 MHz, CDCl$_3$) δ 172.4, 172.0, 171.7, 170.2, 170.1, 136.1, 129.0, 128.0, 127.0, 64.0, 60.3, 53.5, 52.3, 52.1, 48.6, 47.8, 37.8, 29.2, 24.5, 23.2, 19.6. ESI-MS: 477 [M+H]$^+$.

Methyl N^2-(acetyl-L-alanyl)-N^6-((benzyloxy)carbonyl)-L-lysyl-L-prolyl-L-phenylalaninate (5 i). Starting from **8 i** in presence of compound **9**,

ChemMedChem

Research Article
doi.org/10.1002/cmdc.202200050

Chemistry
Europe
European Chemical
Societies Publishing

the title compound was obtained according with general procedure i). Pale yellow amorphous solid, 85% yield. ^{1}H NMR (300 MHz, CDCl$_3$) δ 8.26 (d, $J=8.6$ Hz, 1H), 7.60 (d, $J=7.3$ Hz, 1H), 7.41–6.81 (m, 10H), 6.52–6.47 (m, 1H), 5.86–5.80 (m, 1H), 5.18–4.49 (m, 6H), 3.86–3.37 (m, 5H), 3.21–2.72 (m, 4H), 2.35–1.71 (m, 8H), 1.76–0.93 (m, 8H). ^{13}C NMR (75 MHz, CDCl$_3$) δ 166.8, 166.4, 166.3, 165.6, 164.9, 151.4, 131.7, 131.0, 123.7, 123.1, 122.8, 122.6, 121.5, 61.0, 54.6, 48.4, 46.7, 44.6, 43.2, 42.5, 35.0, 32.8, 26.9, 24.0, 23.6, 19.6, 17.9, 16.3. ESI-MS: 674 [M+Na]$^+$.

Methyl acetyl-L-alanyl-L-lysyl-L-prolyl-L-phenylalaninate (5j). Starting from **5i**, the title compound was obtained according with general procedure v). Pale yellow amorphous solid, 20% yield. ^{1}H NMR (300 MHz, CD$_3$OD) δ 7.43–7.00 (m, 5H), 4.75–4.20 (m, 5H), 3.86–3.70 (m, 1H), 3.63 (s, 3H), 3.35–3.21 (m, 5H), 3.16–2.75 (m, 5H), 2.20–2.10 (m, 1H), 1.82–1.20 (m, 10H). ^{13}C NMR (75 MHz, CD$_3$OD) δ 173.7, 172.9, 171.8, 170.8, 136.4, 129.4, 128.8, 128.1, 127.6, 126.5, 59.8, 54.1, 53.3, 51.1, 50.5, 36.8, 30.4, 29.1, 24.4, 21.6, 20.8, 16.2. ESI-MS: 518 [M+H]$^+$.

Methyl acetyl-L-alanyl-L-histidyl-L-prolyl-L-phenylalaninate (5k). Starting from **10k**, the title compound was obtained according with general procedure ii). Yellow amorphous solid, 62% yield. ^{1}H NMR (300 MHz, CDCl$_3$) δ 8.40–7.65 (m, 3H), 7.62–6.97 (m, 6H), 6.90–6.43 (m, 2H), 5.09–4.28 (m, 4H), 3.83–3.29 (m, 4H), 3.26–2.62 (m, 5H), 2.29–1.39 (m, 7H), 1.43–0.84 (m, 3H). ^{13}C NMR (75 MHz, CDCl$_3$) δ 172.5, 171.8, 170.4, 170.1, 136.4, 135.7, 129.2, 129.0, 128.4, 126.9, 60.3, 53.8, 52.2, 50.8, 48.7, 47.4, 37.5, 29.4, 24.7, 23.1, 19.2. ESI-MS: 527 [M+H]$^+$.

Methyl acetyl-L-alanyl-L-methionyl-L-prolyl-L-phenylalaninate (5l). Starting from **8l** in presence of compound **9**, the title compound was obtained according with general procedure i). Colorless oil, 59% yield. ^{1}H NMR (300 MHz, CDCl$_3$) δ 7.90 (d, J=8.7 Hz, 1H), 7.51–6.77 (m, 6H), 6.37–6.30 (m, 1H), 5.02 (dd, $J=14.1$, 7.9 Hz, 1H), 4.94–4.31 (m, 3H), 3.95–3.44 (m, 5H), 3.31–2.86 (m, 2H), 2.68–2.30 (m, 2H), 2.20–1.80 (m, 11H), 1.20–1.08 (m, 3H). ^{13}C NMR (75 MHz, CDCl$_3$) δ 172.1, 171.7, 171.1, 170.8, 169.9, 136.2, 129.1, 129.0, 128.3, 126.8, 59.8, 53.6, 52.0, 49.1, 48.5, 47.7, 37.8, 32.3, 29.8, 29.6, 28.8, 24.8, 23.2, 19.4, 15.5. ESI-MS: 521 [M+H]$^+$.

Methyl acetyl-L-alanyl-L-glutaminyl-L-prolyl-L-phenylalaninate (5m). Starting from **8m**, the title compound was obtained according with general procedure i) in presence of **9** and subsequent removal of Trt group in acidic conditions according to procedure ii). White amorphous solid, 3% yield. ^{1}H NMR (300 MHz, CDCl$_3$) δ 7.43–6.84 (m, 7H), 6.66 (s, 1H), 5.00–4.67 (m, 1H), 4.54 (dd, $J=7.9$, 2.9 Hz, 1H), 4.39–3.98 (m, 2H), 3.83–3.35 (m, 5H), 3.33–2.88 (m, 2H), 2.52–1.69 (m, 10H), 1.44–0.66 (m, 6H). ESI-MS: 518 [M+H]$^+$.

Methyl 2-(2-acetamidopropanamido)-5-(((benzyloxy)carbonyl)amino)pentanoyl)-L-prolyl-L-phenylalaninate (5n). The title compound was obtained by reacting **8n** and **9** according with general procedure i). White solid, 57% yield. ^{1}H NMR (300 MHz, CDCl$_3$) δ 8.14 (t, $J=22.5$ Hz, 1H), 7.49 (d, $J=7.3$ Hz, 1H), 7.37–6.83 (m, 9H), 6.59 (dd, $J=24.0$, 7.6 Hz, 1H), 5.63–5.35 (m, 1H), 5.33–5.19 (m, 1H), 5.14–4.50 (m, 6H), 3.81–3.36 (m, 5H), 3.22–2.78 (m, 4H), 2.27–1.79 (m, 7H), 1.78–0.97 (m, 7H). ^{13}C NMR (75 MHz, CDCl$_3$) δ 172.1, 171.7, 171.5, 170.8, 170.2, 156.6, 136.8, 136.1, 129.1, 128.9, 128.4, 128.3, 127.9, 127.8, 126.8, 66.2, 59.9, 53.7, 53.4, 52.0, 49.9, 48.4, 47.7, 40.4, 37.9, 29.4, 29.0, 24.8, 24.5, 23.1, 19.7.

Methyl 2-(-2-acetamidopropanamido)-5-aminopentanoyl)-L-prolyl-L-phenylalaninate (5o). Starting from **5n**, the title compound was obtained according with general procedure v). White solid, 89% yield. ^{1}H NMR (300 MHz, CDCl$_3$) δ 8.50 (s, 1H), 8.07 (d, $J=9.7$ Hz, 1H), 7.48 (d, $J=5.6$ Hz, 1H), 7.39–7.00 (m, 5H), 6.84 (d, $J=17.6$ Hz, 1H), 5.12–4.20 (m, 8H), 3.89–3.47 (m, 5H), 3.26–2.57 (m, 4H), 2.42–1.18 (m, 12H). ^{13}C NMR (75 MHz, CDCl$_3$) δ 172.1, 171.8, 170.6, 170.1, 135.7, 129.7, 128.8, 128.6, 127.2, 60.3, 54.5, 52.4, 50.2, 48.2, 47.7, 37.3, 30.3, 29.6, 28.9, 25.2, 23.4, 19.8.

Methyl acetyl-L-alanyl-L-lysyl-D-prolyl-L-phenylalaninate (5p). Starting from **14**, the title compound was obtained according with general procedure v). Colorless oil, 12% yield. ^{1}H NMR (300 MHz, CDCl$_3$) δ 7.51–7.00 (m, 5H), 4.85–4.16 (m, 5H), 3.96–3.70 (m, 1H), 3.53 (s, 3H), 3.25–3.11 (m, 5H), 3.06–2.65 (m, 5H), 2.21–2.11 (m, 1H), 1.92–1.30 (m, 10H). ^{13}C NMR (75 MHz, CDCl$_3$) δ 172.6, 172.3, 171.0, 170.7, 136.4, 130.2, 129.7, 129.2, 128.4, 126.9, 59.9, 53.7, 51.5, 48.6, 47.0, 37.8, 30.9, 28.0, 24.3, 23.1, 22.4, 18.5.

Computational details

Ligands and protein preparations: Peptides were generated using tools available in Maestro (Maestro release 2018, Schrödinger, LLC, New York, NY, 2018) and minimized by MacroModel (MacroModel release 2018, Schrödinger, LLC, New York, NY, 2018) employing OPLSAA 2005 as force field.[28] For simulating the effects derived by the solvent the GB/SA model was employed, selecting "no cutoff" for non-bonded interactions. PRCG technique with 5000 maximum iterations (threshold for gradient convergence = 0.001) was used. The resulting structures were treated by LigPrep (LigPrep release 2018, Schrödinger, LLC, New York, NY, 2018) for identifying the most probable ionization state at cellular pH value (7.4 ± 0.5). The 3D structures of human Pin1 and Pin4 were downloaded from the Protein Data Bank (PDB IDs 2XP4[29] and 3UI5,[30] respectively) and imported in Maestro suite 2018. Water molecules, ions and compounds used for crystallization were removed, while the ligands were kept. The resulting structures were prepared using protein preparation wizard protocol to obtain suitable starting structures for further computational experiments as described previously.[31,32]

Molecular docking studies

Molecular docking investigation was performed using Glide software (Glide release 2018, Schrödinger, LLC, New York, NY, 2018) employing Glide standard precision (SP) method as scoring function as previously performed by us.[33–36] Energy grids were prepared, using the default value of the protein atom scaling factor (1.0 Å), within a cubic box centered on the crystallized ligands. After grid generation, the peptides were docked and the number of docked poses entered to post-docking minimization was set to 5000, and the Glide SP score was evaluated.

Synthesis of R8 conjugated peptides and protein preparation

R8 conjugated peptides were manually synthesized on solid phase on Wang resin (loading 0,3 mmol/g, 125 mg, scale peptide synthesis 0,0375 mmol) following the Fmoc (N-9-Fluorenylmethyloxycarbonyl) strategy and using Oxyma/DIC and HATU/Collidine as coupling agents as reported in the literature.[37]

All the steps of peptide synthesis are briefly reported:

1. 125 mg of Wang resin were swollen with 1 mL of DCM (2 cycles of 30 min).
2. Attachment of the first amino acid on the Wang resin by treatment with 1 mL solution of Fmoc-aa-OH (1 eq), Methylimidazole (0.75 eq) and MSNT (1 eq) in DCM under stirring for 12 h at rt.
3. Acetylation step with a solution of 30% Ac$_2$O and 5% of DIPEA in DMF under stirring for 3 h at rt.
4. Deprotection of the Fmoc protecting group by using a solution of 40% Morpholine, 4% DBU in DMF for 5 min and 20% Morpholine and 2% DBU in DMF for 10 min.

ChemMedChem

Research Article
doi.org/10.1002/cmdc.202200050

**Chemistry
Europe**
European Chemical
Societies Publishing

5. Double coupling steps using first 1 mL solution of Fmoc-aa-OH (1 eq)/Oxyma (1 eq)/DIC (1 eq.) in DMF and then 1 mL solution of Fmoc-aa-OH (1 eq)/HATU (1 eq)/Collidine (2 eq) in DMF, under stirring for 45 min at rt.
6. Cleavage of peptides from the resin by using a mixture of 95% TFA, 2.5% H_2O and 2.5% TIS under stirring for 3 h at rt.

For the esterification of the carboxyl group at the C-terminus, crude peptides were solubilized in CH_3OH at the final concentration of 0.01 M in the presence of $SOCl_2$ (4-fold excess). The reaction was left under stirring for 48 h at rt and monitored by analytical HPLC.

Peptides were purified on a WATERS 2545 preparative system (Waters, Milan, Italy) fitted out with a WATERS 2489 UV/Visible detector, applying a linear gradient of CH_3CN/0.1%TFA in H_2O/0.1% TFA from 5 to 70% of in 15 min, at a flow rate of 15 mL/min on a Jupiter C18 (5 μm, 150×21.2 mm ID) column. MS characterization of the peptide was performed using an ESI-TOF-MS Agilent 1290 Infinity LC System coupled to an Agilent 6230 time-of-flight (TOF) LC/MS System (Agilent Technologies, Cernusco sul Naviglio, Italy). The LC Agilent 1290 LC module was coupled with a photodiode array (PDA) detector and a 6230 time-of-flight MS detector, along with a binary solvent pump degasser, a column heater and an autosampler. LC-MS characterization of the peptide was performed using a C18 Waters xBridge column (3 μm, 4.6×5.0 mm), applying a linear gradient of CH_3CN/0.05%TFA in water 0.05% TFA from 5 to 70% of in 15 min, at a flow rate of 0.2 mL/min. **R8–5i**, LC-MS: 1931.09 $[M+H]^+$; **R8–5k**, LC-MS: 1805.09 $[M+H]^+$. The relative purity of peptides was calculated as the ratio of peak area of the target peptide and the sum of areas of all detected peaks from the UV chromatograms at 210 nm. The purity of all peptides was > 95%. The concentration of the peptides, lacking tryptophan and tyrosine residues was determined via the Scopes method,[38] in which the absorbance of the peptide bond was monitored at 205 nm by NanoDrop200c UV-Vis spectrophotometer. Recombinant His6-tagged-Pin1 and His6-tagged-Pin4 (named Pin1 and Pin4, respectively), were efficiently expressed in BL21(DE3) *E. coli* cells, purified to homogeneity and characterized following protocols reported in literature.[39] Protein concentration was determined by reading the absorbance at 280 nm using a NanoDrop2000c UV-Vis spectrophotometer (Thermo Scientific, USA). For the LC-MS analysis of proteins a C4 Phenomenex (3 μm, 4.6×50 mm) column was used, applying a linear gradient of Solvent B from 15% to 70% in 20 min at a flow rate of 0.2 mL/min. MS analyses were performed under standard mass spectrometry conditions.

Direct binding assays

Binding assays were performed using the Corning Epic label-free technology on the EnSpire Multimode Plate Reader, as previously reported (PerkinElmer, Rodgau, Germany).[40] Briefly, Pin immobilization on the optical biosensors was accomplished by adding 150 μg/ mL protein in 20 mM sodium acetate, pH 5.5, using a 12-channel Thermo Scientific matrix multichannel equalizer pipette followed by overnight incubation at 4°C. The microplate was subsequently washed three times with phosphate-buffered saline (PBS, 0.5% DMSO, pH 7.4) buffer. After the washing steps, samples coated on wells were equilibrated in the assay buffer (PBS, 0.5% DMSO, pH 7.4) for 4 hours (30 μL) and subsequently a baseline was recorded. After another washing step, 15 μL of peptides were dispensed in the plate wells. Peptides were diluted with the assay buffer (PBS, 0.5% DMSO, pH 7.4) at a working concentration of 1 mM (500 μM final concentration in the plate) and then further diluted in the assay buffer directly in a 384-well polypropylene plate for a total of twelve different concentrations. The final readings were taken over a period of 1 h. The difference between the last baseline measurements and the maximum signal was used to determine the KD value. Graphs were generated using GraphPad PRISM® v5.01.

Cell based assays

Cell culture and cell lines: Human Cardiomyocyte AC16, lung carcinoma A549, human colon carcinoma HCT116, breast cancer MCF7 cell lines (purchased from ATCC, Milano, Italy) were cultured in Dulbecco's Modified Eagle Medium (DMEM; EuroClone, Milano, Italy), supplemented with 10% heat-inactivated fetal bovine serum (FBS; Sigma-Aldrich, St Louis, USA) antimicrobials (100 U/mL penicillin, 100 μg/mL streptomycin, 250 ng/mL amphotericin-B), and 2 mM L-glutamine (EuroClone); prostate cancer LNCaP cell line (ATCC) were grown in RPMI 1640 media plus 10%FBS, 100 U/mL penicillin, 100 μg/mL streptomycin, 250 ng/mL amphotericin-B, and 2 mM L-glutamine. The cell lines were routinely checked for mycoplasma contamination.

Antiproliferative assay: Cell viability was determined in AC16, A549, HCT116, MCF7, LNCaP and PNT2 cell lines using Thiazolyl Blue Tetrazolium Bromide [(4,5-dimethylthiazol-2-yl)-2,5-diphenyltetrazolium bromide] (MTT; Sigma-Aldrich) assay, following manufacturer's instructions. Cells were seeded in a 48-well plate at a density of 3×10^4 cells/well and treated, in triplicate, with synthesized peptides at a single concentration of 10 μM for 24 and 48 h. MTT solution was added at 0.5 mg/mL for 3 h, the purple formazan crystals were dissolved in DMSO and absorbance. Absorbance was read at a wavelength of 570 nm with a TECAN M-200 reader (Tecan, Männedorf, Switzerland).

Cell cycle: For cell cycle analyses, HCT116 cells were plated (2×10^5 cells/mL) in multiwells in triplicate and after treatment were harvested with PBS, centrifuged at 1200 rpm for 5 min, and resuspended in 500 μL of a hypotonic solution containing 1×PBS, 0.1% sodium citrate, 0.1% NP-40, RNAase A, and 50 mg/mL PI. After 30 min at room temper-ature (RT) in the dark, samples are acquired on a BD Accuri TM C6 flow cytometer sys-tem (BD Biosciences).

Supporting Information Summary

The Supporting Information contains HPLC and LC-MS analysis of purified **R8–5i** and **R8–5k** peptides, along with representative $^1H/^{13}C$ NMR spectra of compounds **5i** and **5k**.

ChemMedChem

Research Article
doi.org/10.1002/cmdc.202200050

**Chemistry
Europe**
European Chemical
Societies Publishing

Conflict of Interest

The authors declare no conflict of interest.

Data Availability Statement

The data that support the findings of this study are available from the corresponding author upon reasonable request.

[1] B. M. Dunyak, J. E. Gestwicki, *J. Med. Chem.* **2016**, *59*, 9622–9644.
[2] Y. M. Lee, Y.-C. Liou, *Front. Oncol.* **2018**, *8*, 469.
[3] K. P. Lu, X. Z. Zhou, *Nat. Rev. Mol. Cell Biol.* **2007**, *8*, 904–916.
[4] G. M. Wulf, A. Ryo, G. G. Wulf, S. W. Lee, T. Niu, V. Petkova, K. P. Lu, *EMBO J.* **2001**, *20*, 3459–3472.
[5] G. P. Atkinson, S. E. Nozell, D. K. Harrison, M. S. Stonecypher, D. Chen, E. N. Benveniste, *Oncogene* **2009**, *28*, 3735–3745.
[6] G. Sorrentino, M. Mioni, C. Giorgi, N. Ruggeri, P. Pinton, U. Moll, F. Mantovani, G. Del Sal, *Cell Death Differ.* **2013**, *20*, 198–208.
[7] E. S. Yeh, A. R. Means, *Nat. Rev. Cancer* **2007**, *7*, 381–388.
[8] Y. Chen, Y. Wu, H. Yang, X. Li, M. Jie, C. Hu, Y. Wu, S. Yang, Y. Yang, *Cell Death Dis.* **2018**, *9*, 883.
[9] J. Zhang, Y. Nakatsu, T. Shinjo, Y. Guo, H. Sakoda, T. Yamamotoya, Y. Otani, H. Okubo, A. Kushiyama, M. Fujishiro, T. Fukushima, Y. Tsuchiya, H. Kamata, M. Iwashita, F. Nishimura, H. Katagiri, S. I. Takahashi, H. Kurihara, T. Uchida, T. Asan, *J. Biol. Chem.* **2013**, *288*, 20692–20701.
[10] A. Matena, E. Rehic, D. Hönig, B. Kamba, P. Bayer, *Biol. Chem.* **2018**, *399*, 101–125.
[11] S. Stifani, *Biomol. Eng.* **2018**, *8*, 1–14.
[12] V. Frattini, S. M. Pagnotta, Tala, J. J. Fan, M. V. Russo, S. B. Lee, L. Garofano, J. Zhang, P. Shi, G. Lewis, H. Sanson, V. Frederick, A. M. Castano, L. Cerulo, D. C. M. Rolland, R. Mall, K. Mokhtari, K. S. J. Elenitoba-Johnson, M. Sanson, X. Huang, M. Ceccarelli, A. Lasorella, A. Iavarone, *Nature* **2018**, *553*, 222–227.
[13] K. N. Nelson, A. N. Meyer, A. Siari, A. R. Campos, K. Motamedchaboki, D. J. Donoghue, *Mol. Cancer Res.* **2016**, *14*, 458–469.
[14] S. Brogi, S. Maramai, M. Brindisi, G. Chemi, V. Porcari, C. Corallo, L. Gennari, E. Novellino, A. Ramunno, S. Butini, G. Campiani, S. Gemma, *ChemMedChem* **2017**, *12*, 2074–2085.
[15] W. Pu, Y. Zheng, Y. Peng, *Front. Cell Dev. Biol.* **2020**, *8*, 1–11.
[16] T. Uchida, T. Takamiya, M. Takahashi, M. Miyashita, H. Ikeda, H. Terada, T. Matsuo, Y. Shirouzu, M. Yokoyama, S. Fujimori, F. Hunter, *Chem. Biol.* **2003**, *10*, 15–24.
[17] Y. Nakatsu, Y. Matsunaga, K. Ueda, T. Yamamotoya, Y. Inoue, M. Inoue, Y. Mizuno, A. Kushiyama, H. Ono, M. Fujishiro, H. Ito, T. Okabe, T. Asano, *Curr. Med. Chem.* **2018**, *27*, 3314–3329.
[18] W. Bedewy, H. Liao, N. A. Abou-Taleb, S. F. Hammad, T. Nasr, D. Pei, *Org. Biomol. Chem.* **2017**, *15*, 4540–4543.
[19] M. Brindisi, S. Maramai, S. Brogi, E. Fanigliulo, S. Butini, E. Guarino, A. Casagni, S. Lamponi, C. Bonechi, S. M. Nathwani, F. Finetti, F. Ragonese, P. Arcidiacono, P. Campiglia, S. Valenti, E. Novellino, R. Spaccapelo, L. Morbidelli, D. M. Zisterer, C. D. Williams, A. Donati, C. Baldari, G. Campiani, C. Ulivieri, S. Gemma, *Eur. J. Med. Chem.* **2016**, *117*, 301–320.
[20] N. Vale, D. Duarte, S. Silva, A. S. Correia, B. Costa, M. J. Gouveia, A. Ferreira, *Pharmacol. Res.* **2020**, *162*, DOI 10.1016/j.phrs.2020.105231.
[21] D. M. Copolovici, K. Langel, E. Eriste, *ACS Nano* **2014**, 1972–1994.
[22] Y. Shamay, L. Shpirt, G. Ashkenasy, A. David, *Pharm. Res.* **2014**, *31*, 768–779.
[23] N. Vale, D. Duarte, S. Silva, A. S. Correia, B. Costa, M. J. Gouveia, A. Ferreira, W. Bedewy, H. Liao, N. A. Abou-Taleb, S. F. Hammad, T. Nasr, D. Pei, A. Barman, D. Hamelberg, S. Stifani, L. Yang, T. Mashima, S. Sato, M. Mochizuki, H. Sakamoto, T. Yamori, T. Oh-hara, T. Tsuruo, W. Pu, Y. Zheng, Y. Peng, J. Xie, Y. Bi, H. Zhang, S. Dong, L. Teng, R. J. Lee, Z. Yang, K. Murase, K. L. Morrison, P. Y. Tam, R. L. Stafford, F. Jurnak, G. A. Weiss, A. Matena, E. Rehic, D. Hönig, B. Kamba, P. Bayer, K. A. Kromina, A. N. Ignatov, I. A. Abdeeva, K. N. Nelson, A. N. Meyer, A. Siari, A. R. Campos, K. Motamedchaboki, D. J. Donoghue, A. Agents, A. Borrelli, A. L. Tornesello, F. M. Buonaguro, V. Frattini, S. M. Pagnotta, J. J. Fan, V. Marco, S. B. Lee, L. Garofano, J. Zhang, P. Shi, G. Lewis, H. Sanson, V. Frederick, A. M. Castano, L. Cerulo, D. C. M. Rolland, R. Mall, K. Mokhtari, K. S. J. Elenitoba-johnson, M. Sanson, D. M. Copolovici, K. Langel, E. Eriste, P. P. Tripathi, H. Arami, I. Banga, J. Gupta, M. Inoue, Y. Mizuno, A. Kushiyama, H. Ono, M. Fujishiro, J. B. C. Papers, M. Doi, V. Sa, *Org. Biomol. Chem.* **2018**, *8*, 195–202.
[24] L. Yang, T. Mashima, S. Sato, M. Mochizuki, H. Sakamoto, T. Yamori, T. Oh-hara, T. Tsuruo, *Cancer Res.* **2003**, *63*, 831–837.
[25] B. Kaur, M. Kaur, N. Kaur, S. Garg, R. Bhatti, P. Singh, *J. Med. Chem.* **2019**, *62*, 6363–6376.
[26] S. De Cesare, C. A. McKenna, N. Mulholland, L. Murray, D. Bella, D. J. Campopiano, *Org. Biomol. Chem.* **2021**, *19*, 4904–4909.
[27] B. Farina, G. Di Sorbo, A. Chambery, A. Caporale, G. Leoni, R. Russo, F. Mascanzoni, D. Raimondo, R. Fattorusso, M. Ruvo, N. Doti, *Sci. Rep.* **2017**, *7*, 1–13.
[28] W. L. Jorgensen, D. S. Maxwell, J. Tirado-Rives, *J. Am. Chem. Soc.* **1996**, *118*, 11225–11236.
[29] A. Potter, V. Oldfield, C. Nunns, C. Fromont, S. Ray, C. J. Northfield, C. J. Bryant, S. F. Scrace, D. Robinson, N. Matossova, L. Baker, P. Dokurno, A. E. Surgenor, B. Davis, C. M. Richardson, J. B. Murray, J. D. Moore, *Bioorg. Med. Chem. Lett.* **2010**, *20*, 6483–6488.
[30] J. W. Mueller, N. M. Link, A. Matena, L. Hoppstock, A. Rüppel, P. Bayer, W. Blankenfeldt, *J. Am. Chem. Soc.* **2011**, *133*, 20096–20099.
[31] M. Brindisi, J. Senger, C. Cavella, A. Grillo, G. Chemi, S. Gemma, D. M. Cucinella, S. Lamponi, F. Sarno, C. Iside, A. Nebbioso, E. Novellino, T. B. Shaik, C. Romier, D. Herp, M. Jung, S. Butini, G. Campiani, L. Altucci, S. Brogi, *Eur. J. Med. Chem.* **2018**, *157*, 127–138.
[32] A. Di Capua, C. Sticozzi, S. Brogi, M. Brindisi, L. Cappelli, A. Sautebin, A. Rossi, S. Pace, C. Ghelardini, L. Di Cesare Mannelli, G. Valacchi, G. Giorgi, A. Giordani, G. Poce, M. Biava, M. Anzini, *Eur. J. Med. Chem.* **2016**, *109*, 99–106.
[33] L. Testai, E. Piragine, I. Piano, L. Flori, E. Da Pozzo, V. Miragliotta, A. Pirone, V. Citi, L. Di Cesare Mannelli, S. Brogi, S. Carpi, A. Martelli, P. Nieri, C. Martini, C. Ghelardini, C. Gargini, V. Calderone, *Oxid. Met.* **2020**, *2020*, DOI 10.1155/2020/4650207.
[34] M. Paolino, M. Brindisi, A. Vallone, S. Butini, G. Campiani, C. Nannicini, G. Giuliani, M. Anzini, S. Lamponi, G. Giorgi, D. Sbardella, D. M. Ferraris, S. Marini, M. Coletta, I. Palucci, M. Minerva, G. Delogu, I. Pepponi, D. Goletti, A. Cappelli, S. Gemma, S. Brogi, *ChemMedChem* **2018**, *13*, 422–430.
[35] C. C. Maquiaveli, J. F. Lucon-Júnior, S. Brogi, G. Campiani, S. Gemma, P. C. Vieira, E. R. Silva, *J. Nat. Prod.* **2016**, *79*, 1459–1463.
[36] S. Brogi, H. Sirous, V. Calderone, G. Chemi, *Food Funct.* **2020**, *11*, 8122–8132.
[37] A. Caporale, N. Doti, A. Monti, A. Sandomenico, M. Ruvo, *Peptides* **2018**, *102*, 38–46.
[38] R. K. Scopes, *Anal. Biochem.* **1974**, *59*, 277–282.
[39] R. Ranganathan, K. P. Lu, T. Hunter, J. P. Noel, *Cell* **1997**, *89*, 875–886.
[40] B. Farina, M. Sturlese, F. Mascanzoni, A. Caporale, A. Monti, G. Di Sorbo, R. Fattorusso, M. Ruvo, N. Doti, *Biochem. J.* **2018**, *475*, 2377–2393.